Received: 7 April 2022 | Revised: 16 September 2022 | Accepted: 23 October 2022

IET Generation, Transmission & Distribution

DOI: 10.1049/gtd2.12659

The Institution of Engineering and Technology WILEY

ORIGINAL RESEARCH

Optimal adaptive protection of smart grids using high-set relays and smart selection of relay tripping characteristics considering different network configurations and operation modes

Amir Hossein Ataee-Kachoee[1] | Hamed Hashemi-Dezaki[1,2] | Abbas Ketabi[1]

[1]Department of Electrical and Computer Engineering, University of Kashan, 6 km Ghotbravandi Blvd, Kashan, Iran

[2]Research and Innovation Center for Electrical Engineering (RICE), Faculty of Electrical Engineering, University of West Bohemia (UWB), Pilsen, Czech Republic

Correspondence
Hamed Hashemi-Dezaki, Department of Electrical and Computer Engineering, University of Kashan, 6 km Ghotbravandi Blvd, 8731753153 Kashan, Iran.
Email: hamed.hashemi@kashanu.ac.ir

Abstract

Much attention has been paid to optimizing smart grids (SGs) and microgrids (MGs) protection schemes. The SGs' operation in different operating modes (especially grid-connected and islanded conditions) and various system configurations (such as the outage of each of the distribution generations) adversely influence the protection system. The adaptive protection schemes using different setting groups are suitable and reliable solutions to achieve a fast protective system. However, the literature shows a research gap in developing optimized adaptive protection schemes, focusing on constraint reduction, besides the optimal selection of time-current characteristics for direction overcurrent relays (DOCRs) and high-set relays (HSRs). This research aims to fill such a research gap. The power system analyses, such as power flow and short circuit studies, are done in DIgSILENT, and the genetic algorithm (GA) is used to find the optimum solutions. Test results of the IEEE 38-bus distribution system illustrate the advantages of this study compared to existing ones. The comparative test results emphasize that 31.78% and 21.62% decrement in time of the protective scheme in different topologies for the distribution networks of the IEEE 38-bus and IEEE 14-bus test systems could be achievable by simultaneously optimizing relay characteristics and HSRs compared to existing approaches.

1 | INTRODUCTION

The high penetration of renewable and non-renewable distributed generations (DGs) through the concepts of smart grids (SGs) and microgrids (MGs) as future grids has received significant attention in recent years [1–3]. Many benefits can be achieved by deploying DGs in active distribution networks (ADNs) and SGs [4–6]. However, complications have been imposed on the SGs and MGs' control and protection systems due to the integration of DGs into the conventional structure of distribution networks [7, 8]. Hence, several studies in the literature have been devoted to optimizing the protection system of SGs and MGs [9, 10]. The topological evolution of power distribution networks comprising DG units and the islanding capacity of MGs have led to significant changes in the magnitudes of short-circuit currents, consequently affecting the reliability of protection systems in terms of loss of selectivity, sensitivity, and dynamic response [11, 12]. Protection and power quality constraints are the most important issues that limit the maximum penetration of DG in power systems. A change in the short-circuit level due to the presence of DGs might lead to incorrect operation of protective relays and protection miscoordination [13]. Therefore, in [14], using a proposed approach and a new objective function, the location, size, and type of DGs were optimized to maximize DG penetration and protection system speed and reduce power losses. It is essential to develop a protection scheme that works properly in various operating conditions and system configurations and maintains fast without any coordination constraint violation [15, 16]. Changes in the network configuration and various operation modes (grid-connected and islanded modes) of SGs influence the protection system dramatically [17–19].

In some available research works, such as [20], the optimum settings for directional overcurrent relays (DOCRs),

TABLE 1 Literature review summary of SGs' optimal protection

References	Year	Characteristic curve type		Different setting groups	Adaptive protection and reduction of constraints	Different network configurations	Smart selection of characteristic curves	HSRs
		Standard	Non-standard					
[11]	2022	✓	✗	✓	✓	✓	✗	✗
[14]	2022	✓	✗	✓	✓	✓	✗	✗
[17]	2020	✓	✗	✗	✓	✓	✗	✗
[18]	2021	✓	✗	✗	✗	✓	✓	✗
[20]	2017	✓	✗	✗	✗	✓	✗	✗
[22]	2021	✓	✗	✗	✗	✓	✓	✗
[23]	2021	✗	✓	✗	✗	✓	✗	✗
[24]	2022	✗	✓	✗	✗	✓	✗	✗
[32]	2020	✓	✗	✓	✓	✓	✗	✗
[33]	2021	✓	✗	✗	✓	✗	✓	✗
[34]	2021	✓	✗	✗	✓	✓	✓	✗
[35]	2022	✗	✓	✓	✓	✓	✗	✗
[36]	2020	✓	✗	✗	✓	✗	✓	✗
[37]	2022	✓	✗	✓	✓	✓	✗	✗
[39]	2019	✓	✗	✓	✓	✓	✗	✗
[40]	2021	✗	✓	✗	✗	✗	✓	✓
[43]	2016	✗	✓	✗	✗	✗	✓	✗
[44]	2019	✓	✗	✗	✗	✗	✓	✗
[45]	2019	✗	✓	✗	✗	✗	✓	✗
[46]	2020	✓	✗	✗	✗	✗	✗	✗
[47]	2019	✓	✗	✗	✗	✓	✗	✗
[48]	2020	✓	✗	✗	✗	✓	✗	✗
[49]	2014	✗	✓	✗	✗	✓	✗	✗
[50]	2020	✓	✗	✗	✓	✗	✗	✗
[51]	2019	✓	✗	✓	✓	✓	✗	✗
[52]	2019	✓	✗	✗	✗	✗	✓	✗
[53]	2018	✓	✗	✗	✓	✗	✓	✗
[54]	2019	✗	✓	✗	✗	✗	✓	✗
[55]	2018	✓	✗	✗	✗	✗	✗	✗
[56]	2021	✓	✗	✗	✗	✗	✗	✗
[57]	2011	✓	✗	✓	✓	✗	✗	✓
[58]	2006	✓	✗	✓	✓	✗	✗	✗
Proposed method		✓	✗	✓	✓	✓	✓	✓

considering all operation modes and network configurations, have been studied. Although no selectivity constraint violation appears in different conditions, the speed of the protection scheme is adversely affected due to additional limits and constraints. Accordingly, some solutions have been introduced to mitigate the challenges of SGs' protection system, considering all network operation mods only by one setting group [21, 22]. In [23], the dual characteristic curve has been used based on a three-point coordination strategy to protect microgrids and ADNs. In [18, 23], a new optimized communication-free protection scheme has been developed. Although these methods do not require a telecommunication link, the operating time of the relays might increase due to the consideration of one protective setting group for all operating modes. Also, in [24], a new protection scheme has been suggested using dual characteristic overcurrent relays based on $N-1$ contingency.

It should be highlighted that changing from grid connected to islanded mode will impact the short circuit level [25, 26]. Hence, the protection coordination might be adversely affected

TABLE 2 Standard DOCRs' characteristic coefficients [22, 45]

Item	Characteristic curve type	*k*	*n*
1	NI	0.14	0.02
2	VI	13.5	1
3	EI	80	2

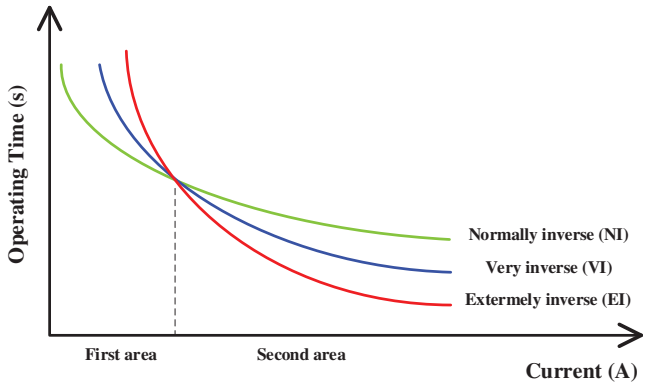

FIGURE 1 Standard characteristics of DOCRs [45]

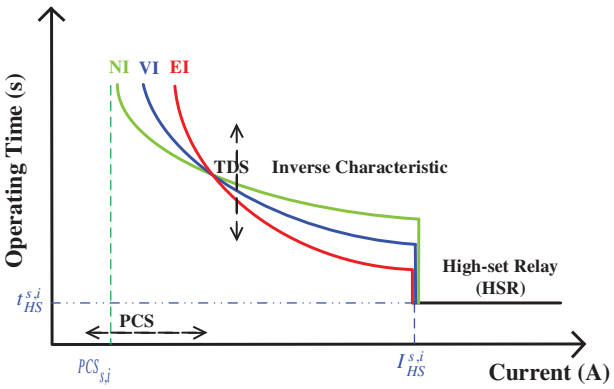

FIGURE 2 Operating time of DOCRs, equipped with HSR [40]

due to changes to islanded modes for ADNs and MGs. Accordingly, islanding detection and appropriate corrective actions in protection settings can be useful [27, 28]. The islanding detection approaches can be divided into two major categories, that is, local and communication-based ones [29, 30]. Different local islanding detection approaches, such as active, passive, and hybrid approaches, have been reported in the literature. The local measurements of voltage, current, and other electrical parameters are used to implement the local islanding detection approaches. These local approaches are suitable from the economic aspects. However, their performance might not be desired in some cases, and non-detection conditions are expected. On the other hand, the communication-based islanding detection approaches are more reliable and effective than local ones. However, the cost of these communication-based and required hardware and software infrastructures would be

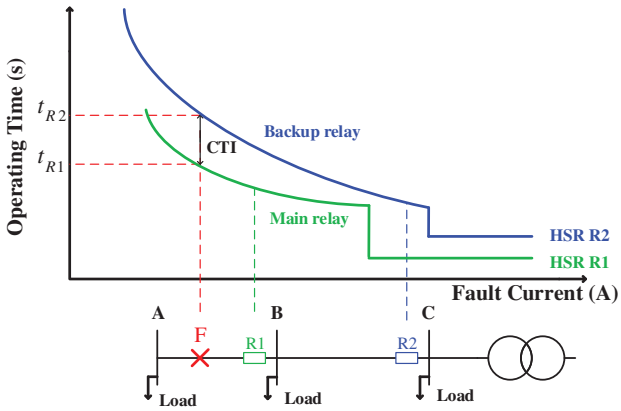

FIGURE 3 Protection coordination between the main and backup DOCRs [17]

considerable. Both discussed islanding approaches (local and communication-based) can be used to change the settings from one group to another. If the communication-based islanding approaches are selected for implementation, comprehensive features will be achievable. Indeed, in communication-based systems, other network configurations are also identified, in addition to islanding detection features. Hence, more than two setting groups and corresponding network configurations have been considered. Using only two setting groups will be helpful if the local islanding detection approaches are utilized to mitigate the challenges in the protection coordination of ADNs, MGs and smart grids due to islanded mode.

To mitigate the operating time challenges of SGs' protection system, considering all network configurations, adaptive protection schemes could be effective alternatives [31, 32]. In [33], a new scheme based on adaptive protection has been reported based on comparing Thevenin impedance in base conditions with the Thevenin impedance measured in other operating conditions. The method presented by Torshizi et al. [33] has several advantages. However, its implementation would be technically complicated due to structural changes in the performance of protection relays. A new adaptive and robust protection scheme was presented in [34], including power quality characteristics and voltage indicators. In [35], using the concept of setting groups (SGs), an adaptive protection scheme was proposed to increase the reliability of the system. Connection and disconnection of switches and DGs result in various scenarios for network topology changes, which have been studied by Mohammadi et al. [35]. Ref. [36] also presented adaptive protection, considering the constraints of DGs' stability. In [37], a new optimal adaptive overcurrent-based protection for large-scale wind farms using a hybrid grey wolf optimizer and rule-based fuzzy logic controller (GWO-FLC) scheme has been reported. The existence of only one setting group for the overcurrent relays (OCRs) would cause drastic miscoordination and false tripping during fault. In order to test the performance of the proposed GWO-FLC scheme, several OCRs based on the standard Schweitzer Engineering Laboratories industrial protection relay (SEL-751) were developed in MATLAB/Simulink. Yousaf

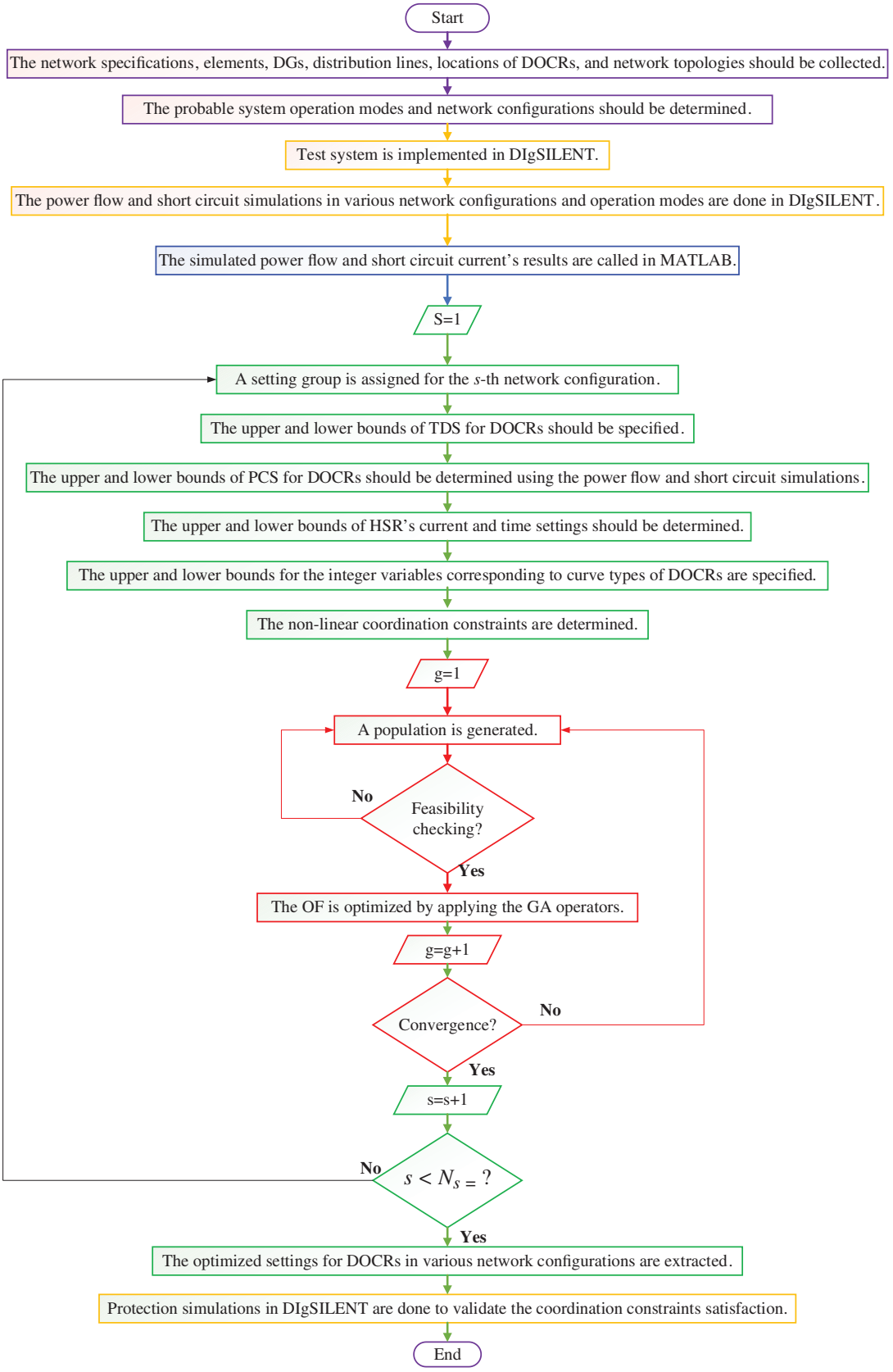

FIGURE 4 Flowchart of optimizing the DOCRs settings based on the proposed optimal adaptive protection method

TABLE 3 Short circuit currents in different configurations

Relay no.	Near-end fault current at the near-end of protection zones in various configurations (A)														
	C_1	C_2	C_3	C_4	C_5	C_6	C_7	C_8	C_9	C_{10}	C_{11}	C_{12}	C_{13}	C_{14}	C_{15}
1	9560	5044	7509	7565	9275	—	8474	7491	9732	9511	9787	9534	9472	5542	9730
2	5667	4527	5490	5521	2400	—	5632	5711	—	5479	—	5652	5527	5930	4626
3	10154	5581	8386	9466	8280	8336	—	7426	10169	10153	10165	9902	10161	6616	10231
4	5810	5272	5054	2787	5623	5693	—	5779	5805	5714	5812	—	5702	5578	5786
5	8980	4490	8586	7620	7172	7007	7103	—	8976	9103	8961	9176	9149	5174	9122
6	6634	6013	3424	5397	6339	6657	6817	—	6570	5570	6591	4647	5436	6684	6365
7	6529	1601	5958	6118	6248	6823	6470	6577	—	—	7230	6466	—	6435	1771
8	3418	3525	3203	3216	2156	2484	3324	3301	—	3533	—	3414	3551	3491	3953
9	7695	2909	7288	7294	6495	7522	7530	7540	—	—	—	7691	8176	7632	3226
10	2796	2668	2292	2543	2652	2774	2813	2527	2863	—	2871	2651	—	2741	2950
11	4593	1338	4233	4334	4424	5016	4551	4630	—	3976	—	4557	3994	4685	1500
12	7029	6332	6511	6530	3820	—	6770	6592	7630	7109	—	7019	7139	6387	7613
13	6278	5382	5936	3090	5919	5966	—	6262	6290	6266	6290	—	6275	5614	6266
14	8655	6396	5412	8055	7767	8170	8500	5060	8644	7883	8663	—	7773	7477	8471
15	9578	7654	6406	7793	8771	8837	9647	6249	9655	10046	9673	8182	—	7995	9804
16	3041	1651	2917	2920	2736	3066	3014	3160	2641	—	2636	3044	—	3125	1823

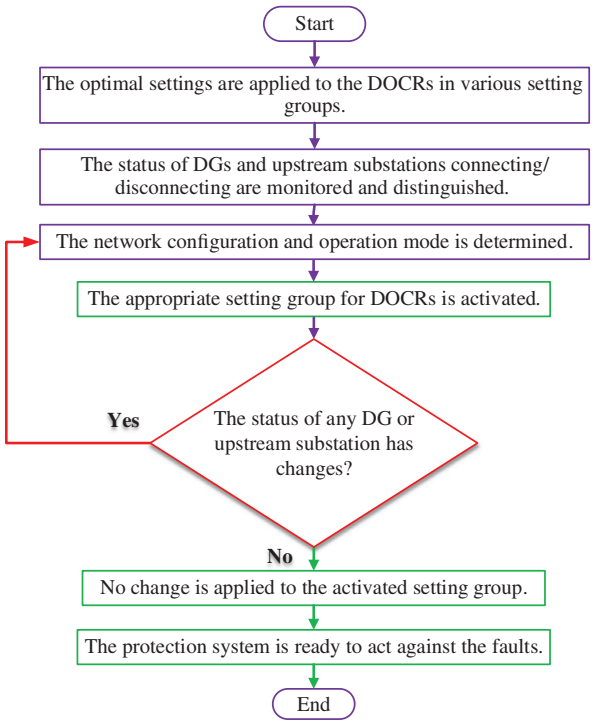

FIGURE 5 Flowchart of implementing the obtained optimized DOCRs settings in test systems based on the monitoring system

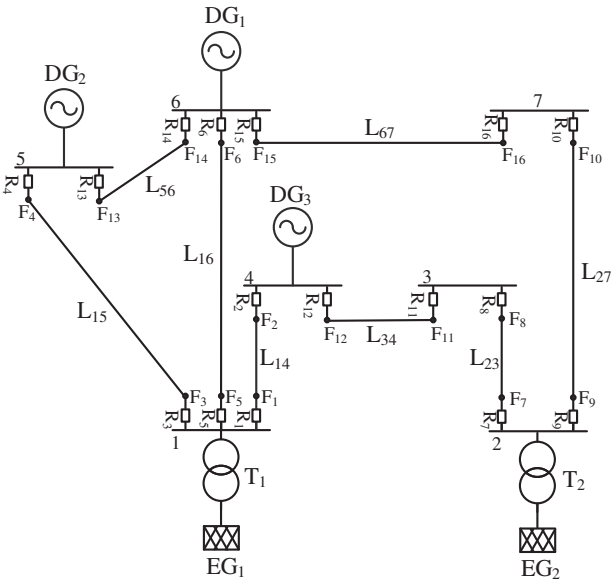

FIGURE 6 Distribution network of the IEEE 14-bus test system [22]

et al. [38] focused on the design of a protection coordination strategy based on the dual-setting directional recloser for the effective implementation of a fuse-saving scheme in distribution networks. Ref. [39] presented an adaptive protection scheme to reduce the constraints of the optimization problem for distinguishing the optimized relay settings and the best operating time of the protection system. Reducing the optimization constraints is one of the crucial factors that make it possible to achieve better results. On the other hand, constraint reduction could be useful to a better search capability in the feasible area of the optimization problem and finding the global optima easier.

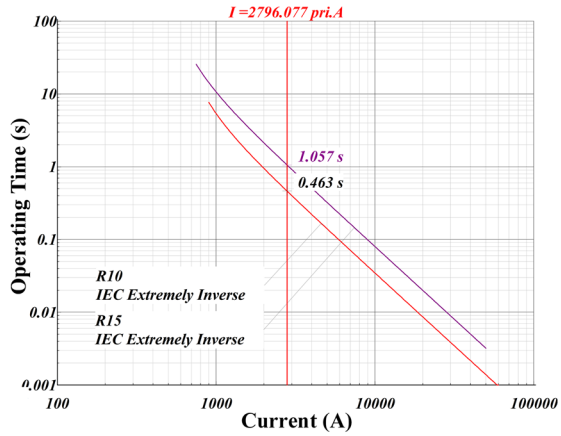

(a) Near-end fault and optimum settings based on the method of [22]

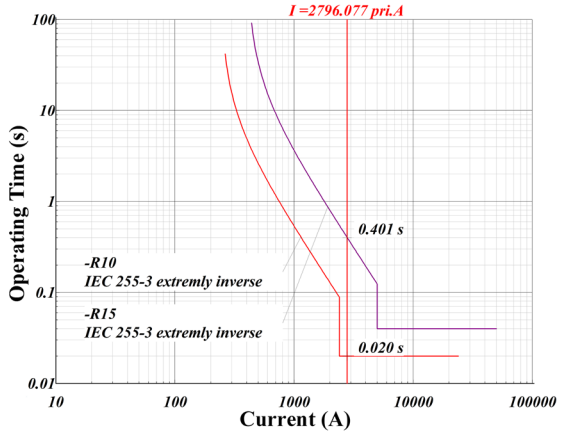

(b) Near-end fault and optimum settings based on the proposed method without limits in the number of setting groups

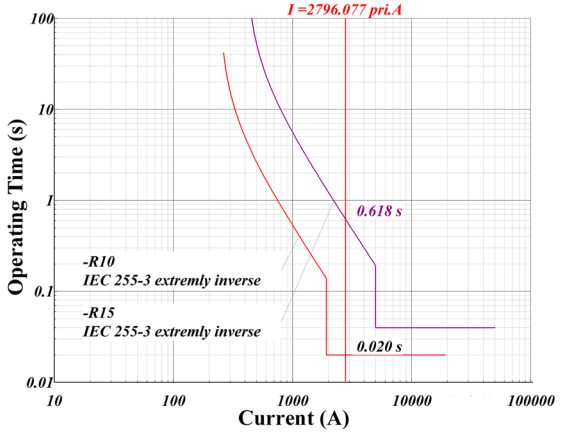

(c) Near-end fault and optimum settings based on the proposed method with limits in the number of setting groups (using three setting groups)

FIGURE 7 Coordination diagrams of R_{10} and R_{15} in C_1 configuration (Grid-connected mode) of the distribution network of the IEEE 14-bus test system. (a) Near-end fault and optimum settings based on the method of [22]. (b) Near-end fault and optimum settings based on the proposed method without limits in the number of setting groups. (c) Near-end fault and optimum settings based on the proposed method with limits in the number of setting groups (using three setting groups)

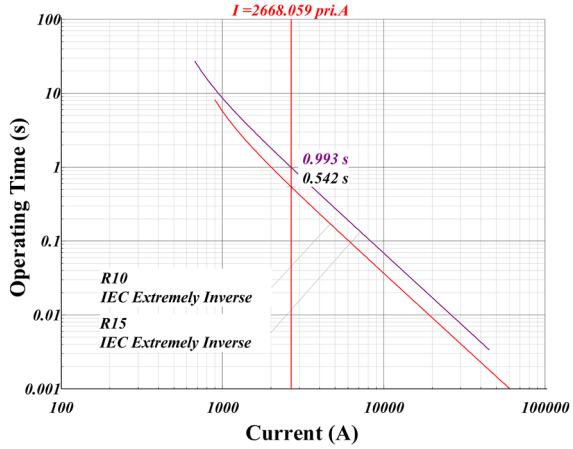

(a) Near-end fault and optimum settings based on the method of [22]

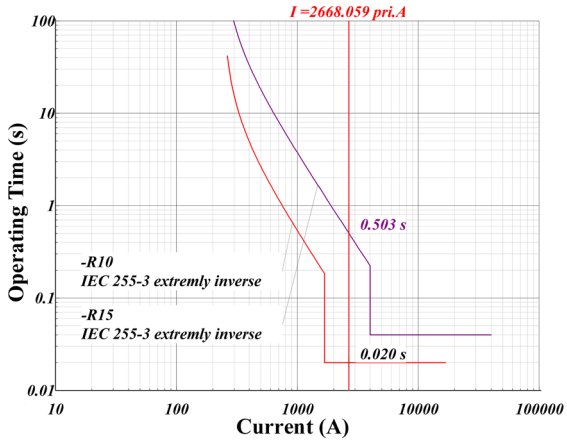

(b) Near-end fault and optimum settings based on the proposed method without limits in the number of setting groups

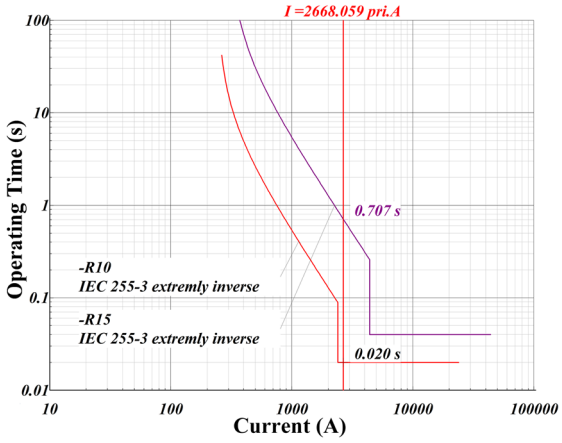

(c) Near-end fault and optimum settings based on the proposed method with limits in the number of setting groups (using three setting groups)

FIGURE 8 Coordination diagrams of R_{10} and R_{15} in C_2 configuration (islanded mode) of the distribution network of the IEEE 14-bus test system. (a) Near-end fault and optimum settings based on the method of [22]. (b) Near-end fault and optimum settings based on the proposed method without limits in the number of setting groups. (c) Near-end fault and optimum settings based on the proposed method with limits in the number of setting groups (using three setting groups)

TABLE 4 Optimal results for different configurations ($N-1$ contingency) based on the proposed method compared to those of [22] and [67] in the distribution network of the IEEE 14-bus test system

	Total relay's operating time (s)		
Configuration no.	Method of [22]	Proposed method without limits in the number of setting groups	Proposed method with limits in the number of setting groups
C_1 (Grid-connected mode)	6.104	4.660	6.233
C_2 (Islanded mode)	12.155	7.285	9.113
C_3 (Outage of DG_1)	7.742	3.616	4.433
C_4 (Outage of DG_2)	7.518	5.045	6.026
C_5 (Outage of DG_3)	7.968	4.825	5.666
C_6 (Outage of L_{1-4})	5.378	3.783	4.195
C_7 (Outage of L_{1-5})	5.375	3.798	4.265
C_8 (Outage of L_{1-6})	6.197	3.778	4.608
C_9 (Outage of L_{2-3})	3.723	2.395	3.604
C_{10} (Outage of L_{2-7})	4.392	2.614	3.755
C_{11} (Outage of L_{3-4})	3.948	3.312	3.998
C_{12} (Outage of L_{5-6})	5.572	5.361	6.539
C_{13} (Outage of L_{6-7})	4.428	2.124	3.368
C_{14} (Outage of EX_1)	6.890	3.444	4.367
C_{15} (Outage of EX_2)	9.934	5.088	6.112
Total operating times of relays in all configurations	97.324	61.127	76.281

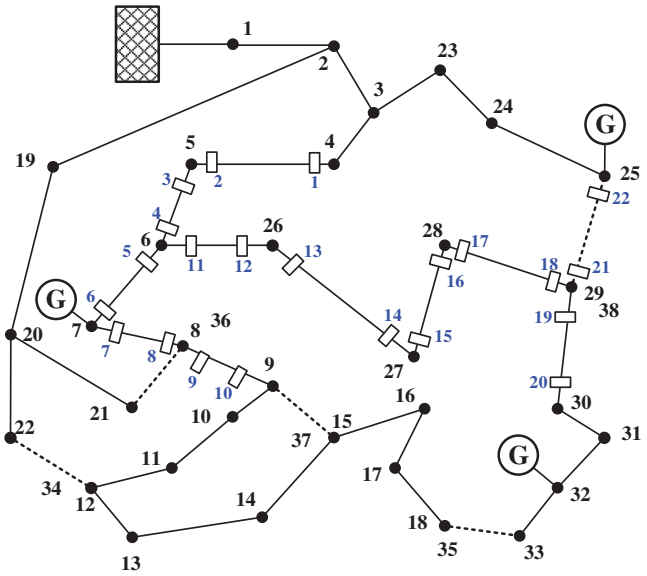

FIGURE 9 SLD of the distribution portion of the IEEE 38-bus test system [39]

TABLE 5 Comparison of the number of constraints for adaptive protection method with and without clustering of network setting groups

Scenario	Number of constraints in the optimization problem	Number of setting groups and separate optimization problems
1	28	1
2	28	1
3	28	1
4	84	1
5	84	1
6	84	1
7	28	3
8	28	3
9	28	3

The optimal selection of DOCRs' characteristics is another solution to improve the adaptive and non-adaptive SGs' protection schemes [40, 41]. Ref. [42] reported a new protection scheme, considering the stability of DGs, while the curve types of DOCRs were optimized. Ahmadi et al. [43] reported an optimization problem for optimizing the protection system, incorporating the optimized relay characteristics. Also, the hyper-sphere search (HSS) algorithm was selected as the optimization algorithm by Ahmadi et al. [43]. The smart selection of standard relay curves for a new double inverse relay model has been presented in [40]. It has been noted that considering the transient stability of synchronous DGs, besides other coordination constraints, adversely affects the speed of the SG's protection system. Hence, introducing a new relay model incorporating the smart selection of relay curves could be helpful. In addition to optimal relay curves' selection, the high-set relays (HSRs) have been used by Narimani and Hashemi-Dezaki [40]. The selection of the optimal curves for DOCRs in a non-adaptive protection scheme, considering different network configurations, has been reported in [22]. The combination of different characteristic curves for overcurrent relays in [44] has also been introduced as a suitable solution to increase the speed of protection designs. The use of non-standard characteristic curves is another issue that has been considered in references, such as [45]. Although optimization of non-standard curves reduces the operating time of the protection system, it will not be possible to implement it in all networks and all overcurrent relays. The non-standard relay curves might not be adequately

TABLE 6 GA parameters and settings

Item	Parameter	Scenario no.								
		1	2	3	4	5	6	7	8	9
1	Number of decision variables	44	66	88	44	66	88	44	66	88
2	Population size	200	200	200	200	200	200	100	100	100
3	Maximum iteration	100	10000	10000	100	10000	10000	100	10000	10000
4	Crossover rate	0.8	0.8	0.8	0.8	0.8	0.8	0.8	0.8	0.8
5	Mutation rate	0.2	0.2	0.2	0.2	0.2	0.2	0.2	0.2	0.2

TABLE 7 Short circuit currents in different modes and network configurations

Relay no.	Short circuit current (I_F) at the near-end of DOCRs in various topologies (A)					
	Topology 1	Topology 2	Topology 3	Topology 4	Topology 5	Topology 6
1	10296	1106	9309	10063	9908	9930
2	3967	1115	2781	3475	3631	3610
3	9051	916	8255	8880	8727	8749
4	7052	1601	5629	6396	6554	6532
5	8339	1108	7358	8310	7816	7910
6	6106	1156	4862	5390	5889	5795
7	7598	1450	6094	6894	7151	7245
8	7206	869	6430	7145	6896	6800
9	11884	1688	10233	11236	11336	11428
10	6089	1130	4976	5810	5718	5625
11	10532	1352	9200	9881	10227	10154
12	2910	754	2173	2869	2526	2599
13	10042	1276	8786	9418	9762	9689
14	3581	857	2742	3505	3163	3236
15	9339	1166	8192	8752	9095	9022
16	6570	1329	5269	6342	5997	6071
17	6295	693	5616	5865	6205	6133
18	8878	1691	7216	8532	8182	8257
19	10615	1327	9337	10085	9932	10547
20	3014	809	2198	2850	2992	2386
21	6356	1039	5305	5911	6394	5710
22	6633	999	5679	6414	5921	6608

TABLE 8 Comparative results of optimal operating times of DOCRs (OF) under various scenarios

Scenario no.	The value of the objective function (s)			
	Base mode	Islanded	Topology 3 (DGs outage)	All modes
1	63.094	81.884	73.197	218.175
2	48.574	73.705	66.141	188.420
3	43.417	60.563	48.317	152.297
4	74.847	93.532	84.673	253.052
5 (like the studies in [22])	66.265	78.437	72.538	217.240
6	48.768	65.036	55.028	168.832
7 (like the studies in [39])	63.094	76.666	71.180	210.940
8	48.574	65.111	61.071	174.756
9	43.417	55.331	45.135	143.883

practical because the standard characteristic curves could only adjust most installed protection relays or new commercial ones. The literature review shows that although optimization of the characteristic curves of OCRs has been discussed in several works, this issue has received less attention in the form of adaptive protection schemes.

Table 1 summarizes the literature review in the field of SGs' optimal protection. As seen, although different studies have been reported based on the optimal selection of relay characteristics, there is a research gap in developing a new adaptive protection scheme for ADNs, MGs and SGs, besides the smart selection of relay curve types. Another research gap is studying the Integration of the HSRs into the adaptive protection scheme of SGs. This study aims to fill such research gaps by developing a new adaptive protection scheme for SGs, considering various network configurations, based on the simultaneously optimized selection of standard relay curves and HSRs. This paper is focused on reducing the selectivity constraints, besides the discussed contributions.

The proposed optimal protection scheme is applied to the IEEE 38-bus test system. The required inputs of the introduced optimization problem, such as power/current passing through the DOCRs and short circuit currents in various network configurations, are extracted using DIgSILENT. The results of the power system studies are exported to MATLAB, and the genetic algorithm (GA) has been selected to find the optimum solutions. Finally, the supplementary protection simulations are performed in DIgSILENT based on optimized solutions and settings to validate the proposed method and selectivity constraints. Moreover, the obtained results are compared to available research works to emphasize the advantages of the proposed method. Comparing test results with non-adaptive

TABLE 9 Coordination constraints violations for various network configurations under different scenarios

Scenario no.	Number of coordination constraints violations			
	Base mode	Islanded	DGs outage	All modes
1	0	9	8	17
2	0	7	7	14
3	0	6	5	11
4	0	0	0	0
5 (like the studies in [22])	0	0	0	0
6	0	0	0	0
7 (like the studies in [39])	0	0	0	0
8	0	0	0	0
9	0	0	0	0

TABLE 10 Optimized settings and operating times of DOCRs under Scenario 1

Main relay	TDS (s)	PCS (A)	Backup relay	Grid-connected		
				MROT (s)	BROT (s)	CTI (s)
1	0.505	21.692	NB	0.870	—	—
2	0.010	21.692	4	0.578	1.621	1.043
3	0.186	23.446	1	0.225	0.570	0.345
4	0.130	23.446	6	1.080	1.679	0.599
4	0.130	23.446	12	1.080	1.589	0.509
5	0.172	42.961	3	0.869	3.096	2.227
5	0.172	42.961	12	0.869	1.376	0.507
6	0.433	42.923	8	0.441	1.789	1.349
7	0.089	73.600	5	1.337	1.905	0.567
8	0.304	73.569	10	0.767	1.700	0.933
9	0.010	29.262	7	0.729	1.589	0.860
10	0.368	29.262	NB	0.328	—	—
11	0.484	16.526	3	0.165	0.788	0.622
11	0.484	16.526	6	0.165	1.402	1.237
12	0.305	16.529	14	0.396	1.145	0.749
13	0.363	14.585	11	0.787	1.410	0.623
14	0.431	14.585	16	0.470	1.712	1.242
15	0.238	12.831	13	0.158	0.488	0.330
16	0.568	12.834	18	1.010	1.905	0.895
17	0.119	11.447	15	0.962	2.440	1.478
18	0.727	11.448	20	0.648	2.200	1.552
18	0.727	11.448	22	0.633	2.477	1.843
19	0.010	93.138	17	1.106	2.806	1.700
19	0.010	93.138	22	1.106	3.035	1.930
20	0.324	93.138	NB	1.438	—	—
21	0.010	89.631	17	0.684	1.729	1.045
21	0.010	89.631	20	0.684	1.647	0.963
22	0.420	89.664	NB	1.411	—	—

schemes using only one setting group and adaptive ones, like [39] that did not use the HSRs and optimized characteristic curves, highlights the novelties of the proposed method. Simulation results show significant improvements by optimizing the relay curves and HSRs in the proposed adaptive protection system. Reducing the coordination constraints and avoiding selectivity constraints violation in different operation modes and network configurations are other advantages of this study, which are examined by test results.

The summary of the major contributions of this study could be noted as follows:

- Simultaneous optimization of time and current settings of DOCRs relays and relay curve types;
- Optimizing the HSRs in the proposed optimal adaptive protection scheme to improve the system protection against significant short circuit currents;
- Considering different operation modes and network configurations in the proposed adaptive optimization method, while the speed of the protection system is desired;
- The outages of DGs are considered in addition to islanded and grid-connected modes;
- Validation of the proposed protective scheme using the DIgSILENT protection studies.

The structure of this article is organized as follows. Section 2 presents the proposed method. In Section 3, simulation results are given. Finally, the conclusion is reported in Section 4.

2 | THE PROPOSED METHOD

As discussed, it is crucial to properly protect the SGs and ADNs using the DOCRs [59, 60]. The satisfaction of protection coordination constraints and the speed of the protection systems are two essential issues that should be simultaneously concerned [61, 62]. The direction and magnitude of short circuit current passing through the distribution lines and corresponding relays are influenced by integrating the DGs into the conventional passive distribution networks [63, 64]. Also, the changes in the network configurations and operation modes are other challenges in the performance of the SG's protective system. For instance, the short circuit current passing through the distribution lines in islanded mode might be less effective than in the grid-connected mode [65, 66]. Therefore, the speed of the protection scheme against the faults in islanded mode and selectivity constraints might be affected for islanded mode.

The conventional protective schemes, considering only the base network configuration, might not be an appropriate solution for ADNs, MG, and SGs [67, 68]. This is mainly because the ADNs, MGs, and SGs, unlike conventional passive distribution networks, are able to work in islanded mode and

TABLE 11 Operating times of DOCRs in islanded mode and Topology 3 under Scenario 1

		Islanded mode (Topology 2)			Topology 3		
Main relay	Backup relay	MROT (s)	BROT (s)	CTI (s)	MROT (s)	BROT (s)	CTI (s)
1	NB	0.851	—	—	0.766	—	—
2	4	1.721	1.897	0.1 75	0.366	0.755	0.389
3	1	0.220	1.233	1.013	0.400	0.990	0.590
4	6	1.707	1.966	0.2 59	1.461	1.572	0.111
4	12	1.707	1.859	0.1 52	1.461	1.722	0.2 61
5	3	0.884	3.622	2.739	0.795	2.898	2.102
5	12	0.884	1.785	0.901	0.795	1.428	0.632
6	8	0.869	2.320	1.452	0.956	2.689	1.734
7	5	2.634	2.852	0.2 18	2.897	3.305	0.408
8	10	0.780	2.205	1.425	0.858	2.555	1.697
9	7	0.720	2.061	1.341	0.792	2.389	1.596
10	NB	0.324	—	—	0.356	—	—
11	3	0.988	1.022	0.0 34	1.087	1.185	0.0 98
11	6	0.988	1.818	0.830	1.087	2.108	1.021
12	14	0.475	0.916	0.441	0.570	0.824	0.2 55
13	11	0.943	1.128	0.1 85	0.962	1.117	0.1 54
14	16	0.563	1.370	0.806	0.676	1.233	0.557
15	13	1.359	1.507	0.1 48	1.250	1.356	0.1 06
16	18	0.998	2.073	1.075	1.197	1.865	0.668
17	15	0.976	2.655	1.678	1.171	2.389	1.218
18	20	2.148	2.394	0.2 46	1.504	1.625	0.1 22
18	22	2.148	2.180	0.0 32	1.504	1.722	0.2 18
19	17	1.637	3.221	1.584	1.224	1.933	0.708
19	22	1.637	3.484	1.847	1.224	2.439	1.215
20	NB	1.459	—	—	1.092	—	—
21	17	0.694	1.985	1.291	0.519	2.338	1.819
21	20	0.694	1.891	1.197	0.519	2.227	1.708
22	NB	1.432	—	—	1.071	—	—

*The relay pairs that do not meet the coordination constraints and minimum CRT have been presented in separate font colours and underline format.

TABLE 12 Optimized settings and operating times of DOCRs under Scenario 2

				Grid-connected		
Main relay	TDS (s)	PCS (A)	CS	Backup relay	MROT (s)	BROT (s)	CTI (s)
1	0.378	170.9	VI	NB	0.340	—	—
2	0.018	21.69	EI	4	0.309	1.373	1.063
3	0.147	31.81	EI	1	0.132	0.506	0.374
4	0.494	81.44	EI	6	0.578	1.421	0.844
4	0.494	81.44	EI	12	0.578	1.345	0.767
5	0.731	219.76	EI	3	0.465	2.621	2.156
5	0.731	219.76	EI	12	0.465	1.116	0.651
6	0.509	95.65	EI	8	0.236	0.668	0.433
7	0.283	118.4	EI	5	0.715	1.612	0.897
8	0.259	74.91	EI	10	0.410	1.439	1.029
9	0.607	29.60	EI	7	0.390	1.345	0.955
10	0.510	29.80	VI	NB	0.176	—	—
11	0.744	271.20	EI	3	0.088	0.879	0.791
11	0.744	271.20	EI	6	0.088	1.187	1.099
12	1.177	40.69	EI	14	0.212	1.589	1.377
13	0.211	160.9	VI	11	0.421	1.194	0.773
14	0.181	130.2	EI	16	0.251	1.449	1.198
15	1.217	38.47	EI	13	0.800	1.167	0.367
16	0.490	97.79	EI	18	0.540	1.612	1.072
17	0.656	24.54	EI	15	0.514	2.066	1.551
18	0.728	109.5	EI	20	0.347	1.863	1.516
18	0.728	109.5	EI	22	0.641	2.097	1.456
19	0.010	93.13	EI	17	0.591	2.375	1.783
19	0.010	93.13	EI	22	0.591	2.513	1.922
20	0.229	96.32	NI	NB	0.769	—	—
21	0.010	90.52	EI	17	0.366	1.618	1.252
21	0.010	90.52	EI	20	0.366	1.387	1.022
22	0.736	90.74	VI	NB	0.755	—	—

other network configurations besides the grid-connected operation mode. Hence, if the coordination constraints regarding the islanded mode and other network configurations would not be concerned with the optimal protection scheme, some miscoordination and coordination constraint violations are expected. The importance of considering various network configurations and corresponding selectivity constraints is emphasized by increasing the penetration of DGs. The modified protective scheme can be helpful, using only one setting group, while various coordination constraints are concerned. However, the feasible area to find the protective settings, considering variable network configurations by applying only one setting group, will be challenging. Hence, much attention has been paid to the adaptive protection schemes based on monitoring the network configuration and status of DGs' connection and upstream substations, considering all network operation modes and topologies [69, 70]. The main purpose of this article is to develop a new adaptive protection scheme, considering various SGs' operation modes and topologies. The DOCRs' time and current settings would be optimized in the proposed study, besides the relay curves and HSRs. This paper also focuses on reducing the coordination constraints of the optimization problem, using the adaptive scheme, and applying separate setting groups for different network configurations.

Various objective functions (OFs) have been reported for SGs in the literature [71, 72]. In some references, only the primary relays' total operating time is considered the OF [17,

TABLE 13 Operating times of DOCRs in islanded mode and Topology 3 under Scenario 2

		Islanded mode (Topology 2)			Topology 3		
Main relay	**Backup relay**	**MROT (s)**	**BROT (s)**	**CTI (s)**	**MROT (s)**	**BROT (s)**	**CTI (s)**
1	NB	0.744			0.659		
2	4	1.504	1.733	0.229	0.250	0.714	0.464
3	1	0.192	1.131	0.938	0.170	0.936	0.766
4	6	0.660	0.795	0.135	1.321	1.487	0.166
4	12	0.660	0.870	0.110	1.321	1.541	0.221
5	3	0.772	3.311	2.538	0.684	2.741	2.057
5	12	0.772	1.631	0.859	0.684	1.351	0.667
6	8	0.759	2.121	1.361	0.822	2.544	1.722
7	5	2.302	2.607	0.305	2.492	3.127	0.635
8	10	0.682	2.015	1.334	0.738	2.417	1.680
9	7	1.630	2.884	1.254	0.681	2.260	1.578
10	NB	2.283			0.307		
11	3	0.864	0.934	0.071	0.935	1.121	0.186
11	6	0.864	1.662	0.798	0.935	1.994	1.059
12	14	0.415	0.837	0.422	0.490	0.780	0.290
13	11	0.825	1.031	0.206	0.828	1.056	0.229
14	16	0.492	1.252	0.759	0.581	1.166	0.585
15	13	1.187	1.377	0.190	1.075	1.283	0.208
16	18	0.872	1.894	1.022	1.030	1.765	0.735
17	15	0.853	2.426	1.573	1.007	1.782	0.775
18	20	1.877	2.188	0.310	1.293	1.537	0.244
18	22	1.877	1.992	0.115	1.293	1.629	0.336
19	17	1.431	2.944	1.514	1.053	1.828	0.775
19	22	1.431	3.185	1.754	1.053	2.307	1.254
20	NB	1.275			0.939		
21	17	0.607	1.814	1.208	0.447	2.212	1.765
21	20	0.607	1.728	1.121	0.447	2.107	1.661
22	NB	1.251			0.921		

*The relay pairs that do not meet the coordination constraints and minimum CRT have been presented in separate font colours and underline format.

34, 36]. Considering the total operating time of the primary and backup relays is another of the most well-known OFs [39, 40]. This paper aims to minimize the total operating time of the primary and backup relays according to (1), subject to coordination constraints. Considering the operating times of DOCRs in various network configurations and operation modes is one of the essential strengths of this research compared to those only focusing on the base network configuration. Moreover, the concerned decision variables and solutions to improve the protection schemes of microgrids and smart grids, such as smart selection of time-current curves and HSRs' settings, besides adaptive schemes, are different from available references.

$$OF = \sum_{s=1}^{N_s} T_s\left(TDS_{s,i}, PCS_{s,i}, CS_{s,i}, I_{s,i}^{HS}, t_{s,i}^{HS}\right) = \sum_{s=1}^{N_s}\left(\sum_{i=1}^{N_p} t_{s,i} + \sum_{j=1}^{N_b} t_{s,j}\right) \quad (1)$$

As shown, the operating time of primary and backup relays in different network configurations are considered in the proposed OF. Also, the time dial settings (TDSs), pick-up current settings (PCSs), curve settings (CSs), the current setting of the HSRs, and the time of HSRs are concerned with the proposed study as decision variables. Moreover, the decision variables corresponding to DOCRs' settings could be different in various network configurations. The operating time of primary and backup relays are calculated using the decision variables and SGs' parameters, such as short circuit current passing through the DOCRs in any network configuration.

The standard characteristics would be assigned to DOCRs. An integer variable has been considered for any DOCRs in a specified network topology. The 1, 2, and 3 values for the discussed integer variable denote that normally inverse (NI), very inverse (VI), and extremely inverse (EI) curves are selected, respectively. The standard characteristic curves of overcurrent relays have different applications, and their coefficients based on IEC 60255 standard and IEEE standards are selected, as shown in Table 2 [73, 74]. Moreover, Figure 1 shows the curves of these standard characteristics for DOCRs.

In (2), it has been presented how the standard curve types and corresponding coefficients are assigned to DOCRs.

$$\begin{bmatrix} k_{s,i} & n_{s,i} \end{bmatrix} = \begin{cases} \begin{bmatrix} 0.14 & 0.02 \end{bmatrix} & If\ CS_{s,i} = 1 \\ \begin{bmatrix} 13.5 & 1.00 \end{bmatrix} & If\ CS_{s,i} = 2 \\ \begin{bmatrix} 80.0 & 2.00 \end{bmatrix} & Otherwise. \end{cases} \quad (2)$$

The DOCRs can be modelled with two or three-stage characteristics [40]. The overcurrent unit includes a low-set stage (I >) and a high-set stage (I > >). For instance, REJ 523 ABB OCR includes the low-set and high-set stages, and more details can be found in the manufacturer's specifications [75]. The high-set overcurrent stage or HSR can operate with instantaneous or definite-time characteristics. The inverse-time function of low-set stage (I >) can be set to be inhibited when high-set stage (I > >) starts. In this case, high-set stage (I > >) will determine the tripping time. In Figure 2, the relay characteristic with two stages (low-set and high-set) has been shown. The HSR facilitates the operating of the DOCRs against the high short circuit current.

In this study, the DOCRs equipped with HSRs are studied. After selecting the characteristic curve for the low-stage, the operating time could be calculated using TDSs, PCSs, time and current settings of HSRs, and fault current passing through the DOCRs, as mathematically expressed in (3) [76]. Figure 2 shows the operating time of any DOCRs, equipped with HSRs, based

TABLE 14 Optimized settings and operating times of DOCRs under Scenario 3

Main relay	TDS (s)	PCS (A)	CS	I_{HS} (A)	Backup relay	Grid-connected		
						MROT (s)	BROT (s)	CTI (s)
1	0.736	60.83	EI	5549	NB	0.188	—	—
2	0.011	22.73	EI	5520	4	0.116	0.416	0.3
3	0.155	25.84	EI	5358	1	0.020	0.470	0.45
4	0.344	97.36	EI	6045	6	0.020	1.873	1.853
4	0.344	97.36	EI	6045	12	0.020	0.926	0.906
5	0.640	63.35	EI	6101	3	0.174	1.060	0.886
5	0.640	63.35	EI	6101	12	0.174	1.471	1.297
6	0.158	132.6	EI	5741	8	0.088	0.881	0.793
7	0.271	117.4	EI	6610	5	0.020	1.787	1.767
8	0.148	317.78	EI	8363	10	0.020	1.896	1.876
9	0.068	29.46	EI	5532	7	0.020	1.772	1.752
10	0.150	51.56	EI	6460	NB	0.066	—	—
11	1.414	140.9	EI	5132	3	0.033	1.767	1.734
11	1.414	140.9	EI	5132	6	0.033	1.564	1.531
12	0.746	50.74	EI	6164	14	0.020	2.094	2.074
13	1.685	167.2	NI	5703	11	0.157	1.981	1.824
14	0.689	67.27	EI	4498	16	0.094	1.910	1.816
15	0.126	85.98	NI	6450	13	0.032	1.658	1.626
16	0.380	249.29	NI	6015	18	0.020	1.761	1.741
17	0.188	45.56	VI	4965	15	0.020	2.415	2.395
18	1.476	259.3	EI	5584	20	0.130	2.455	2.325
18	1.476	259.3	EI	5584	22	0.240	2.763	2.523
19	0.010	93.15	EI	6202	17	0.020	2.148	2.128
19	0.010	93.15	EI	6202	22	0.020	1.718	1.698
20	0.086	108.2	EI	4706	NB	0.288	—	—
21	0.010	89.87	EI	5847	17	0.137	2.132	1.995
21	0.010	89.87	EI	5847	20	0.1137	1.928	1.791
22	0.146	139.8	EI	5549	NB	0.282	—	—

on their settings.

$$t_{s,i} = \begin{cases} TDS_{s,i} \times \left(\dfrac{k_{s,i}}{\left(\dfrac{I^{F}_{s,i}}{PCS_{s,i}} \right)^{n_{s,i}} - 1} \right) & I^{F}_{s,i} \le I^{HS}_{s,i} \\ t^{HS}_{s,i} & I^{F}_{s,i} > I^{HS}_{s,i} \end{cases} \tag{3}$$

The optimization problem should be solved subject to technical limits and constraints. The upper and lower bounds for the TDS and PCS are shown in (4)–(5). The minimum and maximum allowed TDS for DOCRs are determined based on the relay manufacturer's specifications [77, 78]. The maximum and minimum values of the TDS depend on the type and technology of DOCRs [79]. In the upgraded and modernized DOCRs, a wide range of settings could be assigned. On the contrary, a narrow range might exist for non-numeric relays.

$$TDS^{\min}_{s,i} \le TDS_{s,i} \le TDS^{\max}_{s,i} \tag{4}$$

In the proposed optimization problem to find the best settings and solutions for the SG's protective system, PCS's upper and lower bounds should be considered, as demonstrated in (5). Like TDS's upper and lower limits, the PCS has some limits based on the DOCRs' specifications. Also, the minimum allowed PCS should be more than the maximum current passing through the relay. Otherwise, the DOCR operates under normal conditions, which is not desired. Moreover, the minimum fault current passing through the DOCR under each system configuration should be concerned with the upper bounds of the PCS. If the upper bound of the PCS is not considered, the DOCR might not operate against some short circuit faults. In

TABLE 15 Operating times of DOCRs in islanded mode and Topology 3 under Scenario 3

		Islanded mode (Topology 2)			Topology 3		
Main relay	Backup relay	MROT (s)	BROT (s)	CTI (s)	MROT (s)	BROT (s)	CTI (s)
1	NB	0.466	—	—	0.248	—	—
2	4	0.943	1.663	0.721	0.501	1.476	0.975
3	1	0.121	1.085	0.964	0.064	0.962	0.898
4	6	0.933	1.135	0.202	0.495	0.707	0.212
4	12	0.933	1.073	0.140	0.495	0.750	0.256
5	3	0.661	3.177	2.516	0.257	2.818	2.561
5	12	0.661	1.565	0.904	0.468	1.745	1.277
6	8	0.476	2.035	1.559	0.460	1.805	1.346
7	5	1.443	2.501	1.058	0.766	2.219	1.452
8	10	0.427	1.934	1.507	0.227	1.715	1.488
9	7	0.395	1.808	1.413	0.210	1.603	1.394
10	NB	0.178	—	—	0.094	—	—
11	3	0.739	0.896	0.158	0.288	0.560	0.272
11	6	0.739	1.595	0.856	0.288	1.415	1.127
12	14	0.260	0.895	0.635	0.138	0.896	0.758
13	11	0.517	0.757	0.240	0.275	1.103	0.828
14	16	0.309	1.201	0.893	0.164	1.339	1.175
15	13	0.744	0.870	0.125	0.395	0.675	0.279
16	18	0.547	1.818	1.271	0.628	1.613	0.985
17	15	0.535	2.328	1.794	0.614	2.065	1.451
18	20	1.177	2.099	0.923	1.351	1.862	0.511
18	22	1.177	1.463	0.286	1.484	1.696	0.212
19	17	0.897	2.825	1.929	0.476	2.506	2.030
19	22	0.897	3.056	2.159	0.476	1.665	1.188
20	NB	0.799	—	—	0.425	—	—
21	17	0.593	1.741	1.148	0.202	1.544	1.342
21	20	0.593	1.658	1.065	0.202	1.471	1.269
22	NB	1.224	—	—	0.417	—	—

* The relay pairs that do not meet the coordination constraints and minimum CRT have been presented in separate font colours and underline format

TABLE 16 Selectivity constraint violations under Scenarios 1–3

	Islanded			Topology 3		
Scenario	OTM (s)	OTB (s)	CTI (s)	OTM (s)	OTB (s)	CTI (s)
1	R2 1.721	R4 1.897	0.175	R4 1.536	R6 1.572	0.036
	R4 1.706	R6 1.964	0.258	R4 1.536	R12 1.822	0.286
	R4 1.706	R12 1.859	0.153	R11 1.087	R3 1.185	0.098
	R7 2.634	R5 0.1458	0.218	R12 0.570	R14 0.824	0.255
	R11 0.988	R3 2.852	0.034	R13 0.962	R11 1.117	0.154
	R13 0.943	R11 1.128	0.185	R15 1.250	R13 1.356	0.106
	R15 1.359	R13 1.507	0.148	R18 1.504	R20 1.625	0.122
	R18 2.148	R20 2.394	0.246	R18 1.504	R22 1.722	0.218
	R18 2.148	R22 2.180	0.032			
2	R2 1.504	R4 1.733	0.229	R4 1.321	R6 1.487	0.166
	R4 1.662	R6 1.795	0.133	R4 1.321	R12 1.541	0.221
	R4 1.491	R12 1.699	0.208	R13 0.935	R3 1.121	0.186
	R11 0.864	R3 0.934	0.071	R12 0.490	R14 0.780	0.290
	R13 0.825	R11 1.031	0.206	R13 0.828	R11 1.056	0.229
	R15 1.187	R13 1.377	0.190	R15 1.075	R13 1.283	0.208
	R18 1.877	R22 1.992	0.115	R18 1.293	R20 1.537	0.244
3	R4 0.935	R4 1.134	0.199	R4 0.497	R4 0.703	0.206
	R4 0.935	R4 1.073	0.138	R4 0.497	R4 0.750	0.254
	R4 0.739	R4 0.896	0.158	R4 0.288	R4 0.560	0.272
	R4 0.517	R4 0.757	0.240	R4 0.395	R4 0.675	0.279
	R4 0.744	R4 0.870	0.125	R4 1.484	R4 1.696	0.212
	R4 1.177	R4 1.463	0.286			

(6) and (7), it has been explained how the specification limits of DOCRs and other system constraints should be considered in the proposed optimization problem [80, 81].

$$PCS_{s,i}^{\min} \le PCS_{s,i} \le PCS_{s,i}^{\max} \tag{5}$$

$$PCS_{s,i}^{\min} = Max\left\{1.2I_{s,i}^{Load,\max}, PCS^{\min}\right\} \tag{6}$$

$$PCS_{s,i}^{\max} = Min\left\{I_{s,i}^{F,\min}, PCS^{\max}\right\} \tag{7}$$

The upper and lower bounds of the HSR's current settings should be considered in the proposed optimization problem, as shown in (8). The minimum allowed current setting of the HSR should be determined according to the maximum fault current at the end of the protection zone of the understudy DOCR. This is mainly to prevent the mis-coordination between the HSR and the relays located in downstream zones. In addition, the HSR's maximum permitted current setting should be less than the short circuit current value near the protection zone's end. Otherwise, the HSR does not operate for any fault. The technical limits regarding the minimum and maximum HSR setting based on the manufacturer's specifications also should be concerned with the selected upper and lower bounds of HSR's current settings.

$$I_{s,i}^{HS,\min} \le I_{s,i}^{HS} \le I_{s,i}^{HS,\max} \tag{8}$$

The upper and lower bounds of the HSRs time setting could be considered in the proposed optimization problem using (9). In addition to technical limits of HSR based on relay specifications, the HSR's time setting should be equal to or less than the operating time of the corresponding relay by the inverse part of the relay model at the HSR's current setting. In (10), the

TABLE 17 Optimized settings and operating times of DOCRs under Scenario 4

Main relay	TDS (s)	PCS (A)	Backup relay	Grid-connected		
				MROT (s)	BROT (s)	CTI (s)
1	0.606	83.400	NB	1.615	—	—
2	0.010	21.692	4	0.773	1.826	1.053
3	0.102	147.63	1	0.185	0.882	0.697
4	1.871	41.892	6	1.444	1.891	0.447
4	1.871	41.892	12	1.444	2.789	1.345
5	1.783	55.365	3	1.162	3.487	2.325
5	1.783	55.365	12	1.162	1.485	0.323
6	1.827	67.667	8	0.589	0.889	0.300
7	0.689	73.569	5	1.788	2.145	0.357
8	0.924	73.569	10	1.025	1.914	0.889
9	0.010	29.262	7	0.974	1.789	0.815
10	0.151	78.745	NB	0.439	—	—
11	1.991	70.805	3	0.221	1.050	0.829
11	1.991	70.805	6	0.221	1.579	1.358
12	0.162	136.50	14	0.529	1.025	0.496
13	0.378	120.98	11	1.053	1.588	0.535
14	0.212	140.37	16	0.628	0.928	0.300
15	1.939	30.706	13	0.211	0.511	0.300
16	0.496	108.16	18	1.350	2.145	0.795
17	1.534	16.572	15	1.286	2.748	1.462
18	0.224	207.96	20	0.867	2.478	1.611
18	0.224	207.96	22	0.847	2.789	1.942
19	0.010	93.138	17	1.478	3.159	1.681
19	0.010	93.138	22	1.478	3.418	1.940
20	0.049	308.87	NB	1.922	—	—
21	0.010	89.631	17	0.914	1.947	1.033
21	0.010	89.631	20	0.914	1.979	1.065
22	0.806	89.631	NB	1.887	—	—

TABLE 18 Operating times of DOCRs in islanded mode and Topology 3 under Scenario 4

Main relay	Backup relay	Islanded mode (Topology 2)			Topology 3		
		MROT (s)	BROT (s)	CTI (s)	MROT (s)	BROT (s)	CTI (s)
1	NB	0.939	—	—	0.920	—	—
2	4	0.756	2.015	1.259	0.740	1.992	1.252
3	1	0.659	1.314	0.655	0.646	1.299	0.654
4	6	1.413	2.087	0.674	1.383	2.064	0.681
4	12	1.413	1.975	0.563	1.383	1.953	0.570
5	3	1.137	3.848	2.712	1.113	3.805	2.693
5	12	1.137	1.710	0.574	1.113	1.691	0.579
6	8	0.812	2.224	1.412	0.795	2.199	1.404
7	5	1.444	2.368	0.924	1.413	2.341	0.928
8	10	0.850	2.113	1.263	0.832	2.089	1.258
9	7	1.099	1.975	0.876	1.076	1.953	0.877
10	NB	0.823	—	—	0.805	—	—
11	3	0.909	1.749	0.840	0.890	1.887	0.997
11	6	0.909	1.997	1.088	0.890	1.773	0.884
12	14	0.993	2.203	1.210	0.972	1.957	0.984
13	11	1.974	3.418	1.444	1.932	3.035	1.103
14	16	1.179	2.438	1.260	1.154	2.165	1.011
15	13	0.880	1.794	0.914	0.862	1.593	0.731
16	18	2.533	3.700	1.167	0.937	3.286	2.349
17	15	2.413	3.033	0.620	0.892	2.693	1.801
18	20	0.977	2.735	1.757	0.859	2.428	1.569
18	22	0.977	3.079	2.102	0.859	2.734	1.875
19	17	1.194	3.488	2.294	1.050	3.097	2.048
19	22	1.194	3.773	2.578	1.050	3.350	2.300
20	NB	1.553	—	—	1.365	—	—
21	17	1.305	2.149	0.844	1.147	1.908	0.761
21	20	1.305	2.047	0.742	1.147	1.818	0.671
22	NB	1.524	—	—	1.339	—	—

maximum allowed time setting of HSRs has been presented.

$$t_{s,i}^{HS,\min} \le t_{s,i}^{HS} \le t_{s,i}^{HS,\max} \tag{9}$$

$$t_{s,i}^{HS,\max} < TDS_{s,i} \times \left(\frac{k_{s,i}}{\left(\frac{I_{s,i}^{HS}}{PCS_{s,i}} \right)^{n_{s,i}} - 1} \right) \tag{10}$$

The proposed optimization problem should be solved, considering the protective coordination constraints. As shown in (11), a sufficient time interval between the operating time of the main and backup relays in different modes is needed [22, 82]. Figure 3 depicts the coordination constraint and required coordination time interval (CTI) between the primary and backup relays. One of the main advantages of this study is considering the coordination constraints in various network configurations and operation modes. In studies in the field of protective coordination, the minimum CTI has been considered to be between 0.2 and 0.5 s [22, 40]. Here, a value of 0.3 s is assumed for CTI.

$$t_{s,j} - t_{s,i} \ge CTI \qquad \forall s = 1 : N_s \tag{10}$$

Figure 4 shows the step-by-step flowchart of the proposed method to optimize the adaptive protection scheme of SGs and ADNs. As seen, DIgSILENT is used to simulate the understudy SG. The required inputs of the optimization problem, for example, the current passing through the distribution lines in various operation modes (before a fault occurs) and short

TABLE 19 Optimized settings and operating times of DOCRs under Scenario 5

					Grid-connected		
Main relay	TDS (s)	PCS (A)	CS	Backup relay	MROT (s)	BROT (s)	CTI (s)
1	0.290	67.798	EI	NB	0.715	—	—
2	0.087	37.041	EI	4	0.433	1.912	1.479
3	0.690	26.546	EI	1	0.171	0.761	0.590
4	0.246	83.477	EI	6	0.809	1.980	1.171
4	0.246	83.477	EI	12	0.809	1.873	1.064
5	0.534	42.927	EI	3	0.651	3.651	3.000
5	0.534	42.927	EI	12	0.651	1.555	0.904
6	0.620	83.209	EI	8	0.330	0.931	0.601
7	0.411	75.554	EI	5	1.002	2.246	1.244
8	0.039	101.70	VI	10	0.574	2.004	1.430
9	0.157	36.667	EI	7	0.546	1.873	1.327
10	0.050	45.688	EI	NB	0.246	—	—
11	0.596	92.704	EI	3	0.124	0.929	0.805
11	0.596	92.704	EI	6	0.124	1.653	1.529
12	0.391	43.341	EI	14	0.297	1.350	1.053
13	0.417	83.629	EI	11	0.590	1.663	1.073
14	0.316	61.600	EI	16	0.352	2.018	1.666
15	0.609	41.381	EI	13	0.918	1.783	0.865
16	0.484	63.255	EI	18	0.756	2.246	1.489
17	0.156	43.255	EI	15	0.720	2.877	2.157
18	0.237	123.56	EI	20	0.486	2.594	2.109
18	0.237	123.56	EI	22	0.474	2.920	2.446
19	0.018	93.204	EI	17	0.828	3.307	2.479
19	0.018	93.204	EI	22	0.828	3.578	2.750
20	0.022	193.92	NI	NB	1.077	—	—
21	0.014	94.997	EI	17	0.512	2.038	1.526
21	0.014	94.997	EI	20	0.512	1.932	1.420
22	0.353	89.633	NI	NB	1.057	—	—

TABLE 20 Operating times of DOCRs in islanded mode and Topology 3 under Scenario 5

		Islanded mode (Topology 2)			Topology 3		
Main relay	Backup relay	MROT (s)	BROT (s)	CTI (s)	MROT (s)	BROT (s)	CTI (s)
1	NB	0.708	—	—	0.723	—	—
2	4	0.737	1.610	0.873	0.582	1.782	1.201
3	1	0.643	1.298	0.655	0.507	1.162	0.655
4	6	1.065	1.668	0.603	1.087	1.846	0.759
4	12	1.065	1.578	0.513	1.087	1.747	0.660
5	3	0.904	3.075	2.171	0.875	3.404	2.530
5	12	0.904	1.505	0.601	0.875	1.513	0.638
6	8	0.792	1.777	0.985	0.625	1.967	1.342
7	5	1.088	1.892	0.804	1.111	2.095	0.984
8	10	0.829	1.689	0.860	0.654	1.869	1.215
9	7	1.072	1.578	0.506	0.846	1.747	0.901
10	NB	0.738	—	—	0.633	—	—
11	3	0.816	2.064	1.248	0.699	1.688	0.989
11	6	0.816	2.356	1.540	0.699	1.586	0.887
12	14	0.891	2.600	1.708	0.764	1.750	0.986
13	11	1.488	2.732	1.244	1.519	2.715	1.197
14	16	0.889	1.949	1.060	0.907	1.937	1.030
15	13	0.859	1.758	0.899	0.677	1.425	0.748
16	18	1.910	2.957	1.047	0.736	2.940	2.203
17	15	1.819	2.424	0.605	0.701	2.409	1.708
18	20	0.953	2.185	1.232	0.675	2.172	1.497
18	22	0.953	2.460	1.507	0.675	2.446	1.771
19	17	0.950	2.787	1.837	0.825	2.771	1.946
19	22	0.950	3.015	2.065	0.825	2.997	2.172
20	NB	1.171	—	—	1.073	—	—
21	17	0.984	1.717	0.734	0.902	1.707	0.806
21	20	0.984	1.636	0.652	0.902	1.626	0.725
22	NB	1.149	—	—	1.053	—	—

circuit currents, are distinguished by DIgSILENT simulations. The number of considered network configurations and operation modes should be determined. Afterward, the upper and lower bounds of the optimization problems corresponding to various network configurations are selected. The GA solves the proposed optimization problem using DOCRs equipped with HSRs and optimized curve types. The GA is programmed in the MATLAB environment. Furthermore, the obtained results and optimal settings for DOCRs are implemented in DIgsILENT, and protection studies are performed to examine the selectivity constraints and accuracy of the proposed method. Finally, the obtained results could be assigned to DOCRs in practical within different setting groups, and suitable setting groups would be activated according to DG connections and network configurations status.

Figure 5 shows the flowchart for implementing the obtained optimized DOCRs settings in test systems based on the monitoring system. As depicted, the optimized settings within various setting groups are assigned to DOCRs. The statuses of connecting/disconnecting for DGs and upstream substations are monitored, and a suitable setting group is activated for DOCRs. If the status of any DG or upstream substation changes, this change is monitored, and the activated setting group is updated.

The increasing penetration of synchronous and asynchronous DGs has highlighted the transient stability concerns in the ADNs, MGs, and SGs [36, 83]. The DGs are usually low-inertia electrical generators, and the speed of the protection schemes might affect their stability [42, 84]. Hence, besides the selectivity constraints in the proposed study, in future

TABLE 21 Optimized settings and operating times of DOCRs under Scenario 6

Main relay	TDS (s)	PCS (A)	CS	I_{HS} (A)	Backup relay	Grid-connected		
						MROT (s)	BROT (s)	CTI (s)
1	0.585	64.80	EI	8428	NB	0.170	—	—
2	0.030	58.51	VI	7011	4	0.020	1.260	1.240
3	0.782	24.94	EI	7849	1	0.020	0.508	0.488
4	0.267	66.67	EI	7616	6	0.432	1.564	1.132
4	0.267	66.67	EI	7616	12	0.432	1.479	1.047
5	0.299	45.39	EI	8046	3	0.348	2.883	2.535
5	0.299	45.39	EI	8046	12	0.348	1.594	1.246
6	0.122	150.8	NI	9775	8	0.176	1.567	1.391
7	0.131	135.1	NI	7640	5	0.020	1.774	1.754
8	0.209	73.82	EI	8583	10	0.307	1.583	1.276
9	1.225	273.2	VI	6155	7	0.291	1.479	1.188
10	0.108	60.65	NI	7197	NB	0.131	—	—
11	0.553	18.64	EI	7850	3	0.066	1.482	1.416
11	0.553	18.64	EI	7850	6	0.066	1.306	1.240
12	0.549	17.16	VI	8077	14	0.158	1.748	1.590
13	0.439	44.36	NI	8404	11	0.315	1.313	0.998
14	0.945	38.20	EI	8202	16	0.188	1.594	1.406
15	0.171	94.53	NI	6718	13	0.063	1.284	1.221
16	0.320	92.45	EI	6372	18	0.404	1.774	1.370
17	0.226	43.98	EI	6851	15	0.385	2.272	1.887
18	0.374	121.9	EI	6794	20	0.259	2.049	1.790
18	0.374	121.9	EI	6794	22	0.479	2.306	1.827
19	0.017	93.44	EI	7003	17	0.442	2.612	2.170
19	0.017	93.44	EI	7003	22	0.442	2.764	2.322
20	0.401	96.28	EI	7584	NB	0.575	—	—
21	0.018	32.95	EI	8063	17	0.020	1.780	1.760
21	0.018	32.95	EI	8063	20	0.020	1.779	1.759
22	0.404	37.86	NI	7341	NB	0.565	—	—

works, other stability-based constraints can be considered in the optimization problem. The proposed adaptive scheme using the HSRs would be effective in facilitating the satisfaction of selectivity and stability constraints simultaneously.

3 | SIMULATION RESULTS

3.1 | First test system (the distribution network of the IEEE 14-bus test system)

Testing the trustability of the calculations is one of the essential concerns regarding any newly developed method and its programming. Accordingly, one test system (a benchmark case study in [22], as one of the most relevant research works) has been chosen. The introduced method in [22] has been applied to repeat the available outputs. The calculations and programming will be validated if the reported results in the available reference are identical to the obtained results. Moreover, if the comparison of the proposed method is parametric with different references which have the same case study, it is useful to show the performance of the advantages of this study. Thus, the obtained results based on the proposed method are compared with those reported in the available reference.

Figure 6 depicts the distribution grid of the IEEE14-bus test system (the understudy case study in [22]). It has been reported in [22] that the following 15 network configurations based on $N-1$ contingency exist for the distribution grid of the IEEE 14-bus test system:

- Grid-connected (C_1)
- The second configuration, while all upstream substations are out of service or disconnected (islanded mode) (C_2)

TABLE 22 Operating times of DOCRs in islanded mode and Topology 3 under Scenario 6

		Islanded mode (Topology 2)			Topology 3		
Main relay	Backup relay	MROT (s)	BROT (s)	CTI (s)	MROT (s)	BROT (s)	CTI (s)
1	NB	0.723	—	—	0.501	—	—
2	4	0.582	1.364	0.782	0.403	1.403	1.000
3	1	0.508	1.704	1.196	0.351	1.143	0.791
4	6	0.020	1.413	1.393	0.020	1.454	1.434
4	12	0.020	1.516	1.496	0.020	1.376	1.356
5	3	0.769	2.606	1.837	0.606	2.680	2.075
5	12	0.769	1.484	0.715	0.606	1.500	0.894
6	8	0.623	1.930	1.306	0.433	1.950	1.518
7	5	0.020	2.055	2.035	0.020	2.077	2.057
8	10	0.737	2.085	1.348	0.453	1.853	1.400
9	7	0.020	1.949	1.929	0.586	1.732	1.146
10	NB	0.598	—	—	0.438	—	—
11	3	0.660	1.726	1.065	0.020	1.218	1.198
11	6	0.660	1.970	1.310	0.020	1.391	1.371
12	14	0.722	1.912	1.190	0.529	1.535	1.005
13	11	1.434	2.315	0.880	1.052	2.381	1.329
14	16	0.857	1.894	1.037	0.628	1.698	1.070
15	13	0.020	1.575	1.555	0.020	1.249	1.229
16	18	1.714	2.505	0.792	0.834	2.577	1.744
17	15	0.020	2.054	2.034	0.020	2.112	2.092
18	20	0.750	1.852	1.101	0.521	1.905	1.384
18	22	0.750	2.085	1.335	0.521	2.144	1.624
19	17	0.808	2.362	1.554	0.020	2.429	2.409
19	22	0.808	2.554	1.746	0.020	2.627	2.607
20	NB	1.050	—	—	0.827	—	—
21	17	0.883	1.888	1.005	0.695	1.497	0.801
21	20	0.883	1.799	0.916	0.695	1.426	0.730
22	NB	1.031	—	—	0.812	—	—

- Third to fifth configurations, while DGs are disconnected or out of service (C_3–C_5)
- 6th–13th configurations, while any line is out of service (C_6–C_{13})
- 14th–15th configurations, while any upstream substation is disconnected or out of service (C_{14}–C_{15})

3.2 | Simulation results and discussions of the first test system

Table 3 shows the results of short circuit currents in different configurations and operating modes.

To trust the accuracy of computations and programming, DOCRs tripping times by applying the protection scheme of [22] (based on the same setting group in various configurations) have been re-identified, as demonstrated in Table 4. Comparing the obtained results and those reported in [22] infers that the calculations are trustable. Also, the proposed adaptive protection scheme, without limitations in the number of setting groups and with a limited number of setting groups, has been applied to the distribution network of the IEEE 14-bus test system. Table 4 shows the comparison of results based on various schemes. Test results infer that the operation times of the relays in all network configurations due to N−1 contingency have been improved in the proposed method compared to the other two schemes. In the protection scheme based on the proposed method, considering the limits in the number of setting groups, three setting groups have been considered. The first setting group is assigned to the Grid-connected mode (C_1), the second setting group is assigned to the islanded mode (C_2), and the third setting group will support all the remaining modes,

TABLE 23 Optimized settings and operating times of DOCRs in the base configuration under Scenario 7

Main relay	TDS (s)	PCS (A)	Backup relay	Grid-connected		
				MROT (s)	BROT (s)	CTI (s)
1	0.505	21.692	NB	0.870	—	—
2	0.010	21.692	4	0.578	1.621	1.043
3	0.186	23.446	1	0.225	0.570	0.345
4	0.130	23.446	6	1.080	1.679	0.599
4	0.130	23.446	12	1.080	1.589	0.509
5	0.172	42.961	3	0.869	3.096	2.227
5	0.172	42.961	12	0.869	1.376	0.507
6	0.433	42.923	8	0.441	1.789	1.349
7	0.089	73.600	5	1.337	1.905	0.567
8	0.304	73.569	10	0.767	1.700	0.933
9	0.010	29.262	7	0.729	1.589	0.860
10	0.368	29.262	NB	0.328	—	—
11	0.484	16.526	3	0.165	0.788	0.622
11	0.484	16.526	6	0.165	1.402	1.237
12	0.305	16.529	14	0.396	1.145	0.749
13	0.363	14.585	11	0.787	1.410	0.623
14	0.431	14.585	16	0.470	1.712	1.242
15	0.238	12.831	13	0.158	0.488	0.330
16	0.568	12.834	18	1.010	1.905	0.895
17	0.119	11.447	15	0.962	2.440	1.478
18	0.727	11.448	20	0.648	2.200	1.552
18	0.727	11.448	22	0.633	2.477	1.843
19	0.010	93.138	17	1.106	2.806	1.700
19	0.010	93.138	22	1.106	3.035	1.930
20	0.324	93.138	NB	1.438	—	—
21	0.010	89.631	17	0.684	1.729	1.045
21	0.010	89.631	20	0.684	1.647	0.963
22	0.420	89.664	NB	1.411	—	—

TABLE 24 Operating times of DOCRs in islanded mode and Topology 3 under Scenario 7

		Islanded mode (Topology 2)			Topology 3		
Main relay	Backup relay	MROT (s)	BROT (s)	CTI (s)	MROT (s)	BROT (s)	CTI (s)
1	NB	0.781	—	—	0.695	—	—
2	4	0.688	1.787	1.099	0.612	1.583	0.971
3	1	0.427	1.436	1.009	0.380	1.416	1.036
4	6	0.970	1.851	0.881	0.863	1.584	0.721
4	12	0.970	2.082	1.112	0.863	1.782	0.919
5	3	0.780	3.413	2.633	0.694	2.921	2.227
5	12	0.780	1.803	1.023	0.694	1.543	0.849
6	8	0.569	1.972	1.403	1.075	1.688	0.613
7	5	1.201	2.100	0.900	1.068	1.797	0.729
8	10	0.956	2.210	1.254	0.850	1.891	1.041
9	7	0.908	1.907	0.998	0.808	1.632	0.824
10	NB	0.737	—	—	1.392	—	—
11	3	0.812	1.997	1.185	0.965	1.968	1.003
11	6	0.812	1.991	1.179	0.965	1.704	0.739
12	14	1.267	2.005	0.738	1.128	1.796	0.668
13	11	0.944	1.847	0.903	0.840	1.821	0.981
14	16	0.902	2.243	1.341	0.803	1.920	1.117
15	13	0.822	1.880	1.059	1.553	2.444	0.892
16	18	0.907	2.100	1.193	0.807	1.797	0.990
17	15	0.864	2.690	1.826	0.769	2.302	1.534
18	20	0.582	2.425	1.843	0.518	2.076	1.558
18	22	0.582	2.731	2.149	0.518	2.337	1.819
19	17	0.993	3.093	2.100	0.884	2.648	1.764
19	22	0.993	3.346	2.353	0.884	2.864	1.980
20	NB	1.291	—	—	1.149	—	—
21	17	0.614	1.906	1.292	0.547	1.879	1.332
21	20	0.614	1.816	1.201	0.547	1.790	1.243
22	NB	1.267	—	—	1.127	—	—

TABLE 25 Optimized settings and operating times of DOCRs in the base mode under Scenario 8

					Grid-connected		
Main relay	TDS (s)	PCS (A)	CS	Backup relay	MROT (s)	BROT (s)	CTI (s)
1	0.378	170.9	VI	NB	0.340	—	—
2	0.018	21.69	EI	4	0.309	1.373	1.063
3	0.147	31.81	EI	1	0.132	0.506	0.374
4	0.494	81.44	EI	6	0.578	1.421	0.844
4	0.494	81.44	EI	12	0.578	1.345	0.767
5	0.731	219.76	EI	3	0.465	2.621	2.156
5	0.731	219.76	EI	12	0.465	1.116	0.651
6	0.509	95.65	EI	8	0.236	0.668	0.433
7	0.283	118.4	EI	5	0.715	1.612	0.897
8	0.259	74.91	EI	10	0.410	1.439	1.029
9	0.607	29.60	EI	7	0.390	1.345	0.955
10	0.510	29.80	VI	NB	0.176	—	—
11	0.744	271.20	EI	3	0.088	0.879	0.791
11	0.744	271.20	EI	6	0.088	1.187	1.099
12	1.177	40.69	EI	14	0.212	1.589	1.377
13	0.211	160.9	VI	11	0.421	1.194	0.773
14	0.181	130.2	EI	16	0.251	1.449	1.198
15	1.217	38.47	EI	13	0.800	1.167	0.367
16	0.490	97.79	EI	18	0.540	1.612	1.072
17	0.656	24.54	EI	15	0.514	2.066	1.551
18	0.728	109.5	EI	20	0.347	1.863	1.516
18	0.728	109.5	EI	22	0.641	2.097	1.456
19	0.010	93.13	EI	17	0.591	2.375	1.783
19	0.010	93.13	EI	22	0.591	2.513	1.922
20	0.229	96.32	NI	NB	0.769	—	—
21	0.010	90.52	EI	17	0.366	1.618	1.252
21	0.010	90.52	EI	20	0.366	1.387	1.022
22	0.736	90.74	VI	NB	0.755	—	—

that is, the outage of each of the DGs, the outage of each of the lines, and the outage of the upstream substations (C_3–C_{15}). So, in the case of considering all the topologies and operation modes due to $N-1$ contingency, the total operating times of the relays have decreased by 21.62% and 37.19 % by applying the proposed method with/without limits in the number of setting groups compared to the protective schemes of [22], respectively.

In addition to comparing the obtained results with other available references in the same case study, the DIgSILENT protection simulations based on optimized settings have been done to guarantee the trustability of the computations and programming. For a typical representation of DIgSILENT simulations, the coordination diagrams of R_{10} and R_{15} in C_1 (Grid-connected mode) and C_2 (Islanded mode) configurations for near-end faults are depicted in Figures 7 and 8. As revealed by test results, the coordination constraints have been satisfied for all studied schemes.

3.3 | Second test system (the distribution portion of the IEEE 38-bus test system)

The proposed method has been applied to the distribution portion of the IEEE 38-bus test system. Figure 9 shows the single line diagram (SLD) of the test system [39]. The voltage level of the understudy test system is 12.66 kV with 33 buses and 5 manoeuvre lines. If the manoeuvre lines are in the open position, the network will be radial, and if the manoeuvre lines are closed, the network will be able to operate as an interconnected ring network. Here, the protective coordination of the network in the closed condition of all manoeuvre lines will be studied.

TABLE 26 Operating times of DOCRs in islanded mode and Topology 3 under Scenario 8

		Islanded mode (Topology 2)			Topology 3		
Main relay	**Backup relay**	**MROT (s)**	**BROT (s)**	**CTI (s)**	**MROT (s)**	**BROT (s)**	**CTI (s)**
1	NB	0.589	—	—	0.546	—	—
2	4	0.671	1.428	0.757	0.481	1.416	0.935
3	1	0.417	1.419	1.003	0.299	1.266	0.968
4	6	0.731	1.479	0.748	0.678	1.417	0.739
4	12	0.731	1.664	0.933	0.678	1.594	0.916
5	3	0.621	2.728	2.107	0.546	2.613	2.068
5	12	0.621	1.586	0.966	0.546	1.380	0.835
6	8	0.555	1.576	1.021	0.845	1.510	0.665
7	5	0.905	1.678	0.773	0.840	1.608	0.768
8	10	0.932	1.766	0.834	0.668	1.692	1.024
9	7	0.886	1.524	0.638	0.635	1.460	0.825
10	NB	0.661	—	—	1.094	—	—
11	3	0.729	2.356	1.627	0.759	1.761	1.002
11	6	0.729	2.349	1.620	0.759	1.524	0.766
12	14	1.137	2.366	1.228	0.886	1.606	0.720
13	11	0.712	1.476	0.764	0.660	1.629	0.968
14	16	0.680	1.793	1.112	0.631	1.718	1.086
15	13	0.801	1.843	1.041	1.220	2.187	0.966
16	18	0.684	1.678	0.995	0.634	1.608	0.974
17	15	0.651	2.150	1.498	0.604	2.060	1.455
18	20	0.568	1.938	1.371	0.407	1.857	1.450
18	22	0.568	2.182	1.615	0.407	2.091	1.684
19	17	0.790	2.472	1.682	0.695	2.369	1.674
19	22	0.790	2.674	1.884	0.695	2.562	1.867
20	NB	0.973	—	—	0.903	—	—
21	17	0.463	1.523	1.060	0.430	1.681	1.251
21	20	0.463	1.451	0.988	0.430	1.601	1.171
22	NB	0.955	—	—	0.886	—	—

In the studied network, 3 DGs have been installed in buses 7, 25, and 31. The capacity of each of the mentioned DGs is considered to be 3 MVA. 22 DOCRs are used to protect this system, which is located at the beginning and end of distribution lines. The locations of DOCRs have been depicted in Figure 9. Each relay might have 1 or 2 backup relays. Hence, in this test system, 28 pairs of DOCRs should be considered to satisfy the coordination constraints.

The distribution portion of the IEEE 38-bus test system has been simulated in DIgSILENT to perform the power flow and short circuit studies. Then, the GA has been programmed in the MATLAB environment to optimize the protection coordination problem.

The following topologies are considered in the proposed optimal protection scheme:

- Topology 1 (Base grid-connected mode): All DGs and upstream substations are available in base mode.
- Topology 2 (Islanded mode): All DGs are available, while the upstream grids and substations are out-of-service.
- Topology 3: All DGs are disconnected, and only upstream grids and substations supply the distribution system.

It should be noted that the limits in the number of setting groups of DOCRs should be concerned with the optimal protection schemes. Hence, the above operation modes have been considered, which are more probable. If the number of DOCRs' setting groups is more than 3, or it is possible to change the protection settings dynamically, the following additional topologies could be considered:

- Topology 4: All DGs and external grids are available except the DG unit installed in Bus 7.
- Topology 5: All DGs and external grids are available except the DG unit installed in Bus 25.
- Topology 6: All DGs and external grids are available except the DG unit installed in Bus 31.

Clustering the topologies and operation modes of SGs, including $N-1$ contingency, in the proposed adaptive protective scheme can be considered for future work.

3.4 | Various studied scenarios for the second test system

The following scenarios based on non-adaptive and adaptive approaches, considering and neglecting the changes in network configurations, optimizing the relay curves, and using the HSRs are studied:

- Scenario 1: A non-adaptive protection scheme is used. Also, the protective settings are optimized, while only the base network configuration and corresponding coordination constraints are concerned. The HSRs are not used in this scenario, and the pre-defined relay curves are assigned to DOCRs.
  Scenario 2: A non-adaptive protection scheme is used. Also, protective settings are optimized, while only the base network configuration and corresponding coordination constraints are concerned. The HSRs are not used in this scenario, while the relay curves are optimized.
  Scenario 3: A non-adaptive protection scheme is used. Also, protective settings are optimized, while only the base network configuration and corresponding coordination constraints are concerned. The HSRs are used in this scenario while the relay curves are optimized.
  Scenario 4: A non-adaptive protection scheme is used. Also, protective settings are optimized, considering different network configurations and operation modes. The HSRs are not used in this

TABLE 27 Optimized settings and operating times of DOCRs in base grid-connected mode (Topology 1) under Scenario 9

Main relay	TDS (s)	PCS (A)	CS	I_{HS} (A)	Backup relay	Grid-connected		
						MROT (s)	BROT (s)	CTI (s)
1	0.736	60.83	EI	5549	NB	0.188	—	—
2	0.011	22.73	EI	5520	4	0.116	0.416	0.3
3	0.155	25.84	EI	5358	1	0.020	0.470	0.45
4	0.344	97.36	EI	4870	6	0.020	1.873	1.853
4	0.344	97.36	EI	4870	12	0.020	0.926	0.906
5	0.640	63.35	EI	6101	3	0.174	1.060	0.886
5	0.640	63.35	EI	6101	12	0.174	1.471	1.297
6	0.158	132.6	EI	8150	8	0.088	0.881	0.793
7	0.271	117.4	EI	6610	5	0.020	1.787	1.767
8	0.148	317.78	EI	6763	10	0.020	1.896	1.876
9	0.068	29.46	EI	5532	7	0.020	1.772	1.752
10	0.150	51.56	EI	6460	NB	0.066	—	—
11	1.414	140.9	EI	5132	3	0.033	1.767	1.734
11	1.414	140.9	EI	5132	6	0.033	1.564	1.531
12	0.746	50.74	EI	6164	14	0.020	2.094	2.074
13	1.685	167.2	NI	5703	11	0.157	1.981	1.824
14	0.689	67.27	EI	4498	16	0.094	1.910	1.816
15	0.126	85.98	NI	6450	13	0.032	1.658	1.626
16	0.380	249.29	NI	6015	18	0.020	1.761	1.741
17	0.188	45.56	VI	4965	15	0.020	2.415	2.395
18	1.476	259.3	EI	5584	20	0.130	2.455	2.325
18	1.476	259.3	EI	5584	22	0.240	2.763	2.523
19	0.010	93.15	EI	6202	17	0.020	2.148	2.128
19	0.010	93.15	EI	6202	22	0.020	1.718	1.698
20	0.086	108.2	EI	4706	NB	0.288	—	—
21	0.010	89.87	EI	5847	17	0.137	2.132	1.995
21	0.010	89.87	EI	5847	20	0.1137	1.928	1.791
22	0.146	139.8	EI	5549	NB	0.282	—	—

scenario, and the pre-defined relay curves are assigned to DOCRs.

Scenario 5: A non-adaptive protection scheme is used. Also, protective settings are optimized, considering different network configurations and operation modes. The HSRs are not used in this scenario, while the relay curves are optimized. The studies under Scenario 5 will be like those in [22].

Scenario 6: A non-adaptive protection scheme is used. Also, protective settings are optimized, considering different network configurations and operation modes. The HSRs are used in this scenario while the relay curves are optimized.

Scenario 7: An adaptive protection scheme is used. Also, protective settings are optimized, considering different network configurations and operation modes. The HSRs are not used in this scenario, and the pre-defined relay curves are assigned to DOCRs. The studies under Scenario 5 will be like those in [39].

Scenario 8: An adaptive protection scheme is used. Also, protective settings are optimized, considering different network configurations and operation modes. The HSRs are not used in this scenario, while the relay curves are optimized.

Scenario 9: The proposed adaptive protection scheme is used. Also, protective settings are optimized, considering different network configurations and operation modes. The HSRs are used in this scenario while the relay curves are optimized.

In Table 5, the number of selectivity constraints under various scenarios has been presented. As seen, the number of coordination constraints would increase due to considering

TABLE 28 Optimized settings and operating times of DOCRs in islanded mode (Topology 2) under Scenario 9

Main relay	TDS (s)	PCS (A)	CS	I_{HS} (A)	Backup relay	Islanded mode (Topology 2)		
						MROT (s)	BROT (s)	CTI (s)
1	0.347	53.47	EI	1341	NB	0.358	—	—
2	0.010	24.53	EI	1334	4	0.529	1.210	0.681
3	0.073	227.15	EI	1295	1	0.020	1.863	1.843
4	0.162	85.58	EI	1219	6	0.020	1.253	1.233
4	0.162	85.58	EI	1219	12	0.020	1.598	1.578
5	0.302	55.68	EI	1474	3	0.528	2.311	1.783
5	0.302	55.68	NI	1474	12	0.528	1.983	1.455
6	0.074	116.56	EI	3590	8	0.556	2.169	1.614
7	0.128	103.19	EI	1597	5	0.020	2.310	2.290
8	0.070	279.86	VI	1634	10	0.829	2.181	1.352
9	0.032	25.90	EI	1337	7	0.020	1.882	1.862
10	0.071	45.32	EI	1561	NB	0.643	—	—
11	0.666	123.85	EI	1240	3	0.020	1.970	1.950
11	0.666	123.85	EI	1240	6	0.020	1.965	1.945
12	0.352	44.60	EI	1489	14	0.921	1.740	0.819
13	0.794	146.97	NI	1378	11	0.020	1.788	1.768
14	0.325	59.13	EI	1087	16	0.656	1.742	1.087
15	0.059	75.58	NI	1558	13	0.020	1.650	1.630
16	0.179	219.12	NI	1453	18	0.614	2.032	1.419
17	0.089	40.05	VI	1200	15	0.020	1.821	1.801
18	0.695	227.92	EI	1349	20	0.568	1.642	1.074
18	0.695	227.92	EI	1349	22	0.568	1.849	1.281
19	0.015	81.88	EI	1499	17	0.020	2.095	2.075
19	0.015	81.88	EI	1499	22	0.020	2.265	2.245
20	0.129	95.11	NI	1137	NB	0.874	—	—
21	0.015	79.00	EI	1413	17	0.533	1.883	1.350
21	0.015	79.00	EI	1413	20	0.533	1.794	1.261
22	0.138	122.88	NI	1341	NB	0.857	—	—

the different network configurations. On the other hand, it is inevitable to neglect the various configurations because some coordination constraints might happen. The results in Table 5 show that the adaptive protection scheme could be an appropriate alternative for optimal protection coordination of SGs, considering different configurations, while the number of selectivity constraints does not increase.

One of the crucial issues in solving optimization problems by meta-heuristic algorithms is to ensure optimal global solutions and the reproducibility of problem-solving [22, 40]. Therefore, the proposed optimization problem for different scenarios has been run ten times to ensure the optimal global solution. The results presented are based on the best results obtained. In addition, statistical studies have shown optimization problem solving, reproducibility, and acceptable standard deviation in the final optimal solutions. In addition, the settings of the genetic algorithm are determined based on the sensitivity analysis based on convergence and the optimality criteria. Table 6 presents the selected settings for the GA to solve the proposed optimization problem under various scenarios.

3.5 | Test result for the second test system

Table 7 shows the results of short circuit currents in different operating modes and network configurations. Test results infer that changes in the magnitude of short circuit current passing through the DOCRs in various network topologies are considerable that might affect the protection schemes.

Table 8 shows the optimum values of the OF, including the operating times of main and backup relays, under various scenarios. There is one set of settings under Scenarios 1–6, and the operating times of DOCRs in islanded mode and Topology 3 are calculated using the discussed settings. There are different

settings for grid-connected mode, islanded mode, and Topology 3 under Scenarios 7–9. Moreover, the coordination constraint violations under various scenarios are described in Table 9.

The comparative analyses show that the protection system under Scenarios 1–3 might not work properly in islanded mode and Topology 3. This is mainly because of neglecting the selectivity constraints under these scenarios. The number of coordination constraint violations under Scenarios 1–3 is considerable, which illustrates the importance of considering different topologies in the protection scheme of smart grids.

The problem of coordination constraint violations has been solved under Scenarios 4–6. However, the operating times of DOCRs have increased. It is concluded that a 15.98% increment in the operating time of the protection system appears due to considering different network configurations (Comparison of Scenarios 2 and 5). Although the speed of the protection scheme is influenced by considering various network configurations and their constraints, these schemes would be better than conventional ones with considerable coordination constraint violations.

The advantages of the proposed adaptive protective scheme have been highlighted according to comparative test results. Test results infer that the operating time and speed of the protection schemes under Scenarios 7–9 have been improved while there is no coordination constraint violation. The comparative test results between the proposed method (Scenario 9) and Scenario 5 (like the studies in [22]) show a 33.76% improvement in the speed of the protective scheme by applying the proposed adaptive scheme using the HSRs and optimal curve selection.

As revealed by test results, the smart selection of relay curves is an effective solution to improve the speed of the protection system. Regardless of the non-adaptive and adaptive schemes, optimizing the relay characteristics has improved the operating time of DOCRs. Furthermore, the HSRs are good solutions to decrease the operating time of DOCRs and the protective scheme of smart grids.

Test results imply that a 17.15% improvement in operating time of DOCRs appears by optimizing the relay characteristics under Scenario 9 compared to Scenario 8. Also, a 31.78% decrement in time of the protective scheme in different topologies could be achievable by simultaneous optimization of relay characteristics and HSRs under Scenario 9 (the proposed method) compared to Scenario 7 (like the studies in [39]), which is an adaptive protection scheme with pre-defined relay characteristics and without HSRs.

Table 10 presents the optimized time dial settings and pick-up current settings of DOCRs under Scenario 1. As noted, under Scenario 1, only the base configuration (grid-connected mode, including all DGs) is considered. As seen, the main relay operating time (MROT), backup relay's operating time (BROT), and CTI for various fault locations imply that the selectivity constraints have been met.

The optimal total operating times of main and backup relays for the base configuration under Scenario 1 is 63.094 s. If the optimal DOCRs' settings are determined according to the base configuration (under Scenario 1), the operating time of main and backup relays in islanded mode and Topology 3 would be as shown in Table 11. The relay pairs that do not meet the coordination constraints and minimum CRT have been presented in separate font colours and underline format. Test results infer that some coordination constraint violations occur in other network topologies. Test results imply that considering various network configurations and operation modes is necessary to determine the optimum relay settings. Otherwise, coordination constraint violations are inevitable. The reason for the violation of such constraints is that under Scenarios 1–3, only the base mode of the network has been considered, and other modes and network topologies have not been concerned with the optimization problem. The total operating times of DOCRs in islanded mode (Topology 2) and Topology 3, using the optimal settings under Scenario 1, would be 81.884 and 73.197 s, respectively. The speed of the protection scheme in Topologies 2 and 3 is less than the base grid-connected mode. This is mainly expected because of the short circuit current through the DOCRs' decrement in islanded mode and the outage of DGs. However, the coordination constraint violation will not be acceptable.

Figure 10 shows the coordination diagrams of two typical relays (Relays 4 and 6) based on DIgSILENT protection studies in the base grid-connected mode, islanded mode, and Topology 3. The protection studies in DIgSILENT approve the obtained results presented in Table 11. It is concluded that a mis-coordination might appear between these discussed relays in the islanded mode and Topology 3 under Scenario 1.

Table 12 demonstrates the optimized current and time settings of DOCRs under Scenario 2. Also, the optimal characteristic curves for DOCRs have been presented in Table 12. Comparing the obtained test results under Scenarios 1 and 2 illustrates the advantages of smart selection of characteristic curves for DOCRs. The total operating times of DOCRs under Scenario 2 would be 48.574 s, which is 14.52 s (23.01%) less than Scenario 1. Test results approve the advantages of optimizing the characteristic curves. If the optimized settings of DOCRs under Scenario 2 are applied to the understudy test system, the operating times of main and backup relays in islanded mode and Topology 3 would be as shown in Table 13. As revealed by test results, it is inferred that all selectivity constraints might not be satisfied by applying the obtained solutions under Scenario 2.

Figure 11 shows the protection studies in DIgSILENT according to optimized settings under Scenario 2 for two typical relays (4 and 6) in various topologies. A similar problem with Scenario 1 also appears under Scenario 2. The sufficient coordination time intervals have not been satisfied for Relays 4 and 6 in islanded mode and Topology 3 under Scenario 2.

Test results under Scenario 3 are shown in Table 14. The optimized settings for DOCRs, including time and current settings for inverse characteristics, types of time–current curves, and HSR settings, under Scenario 3 have been demonstrated. The results under Scenario 3 have been obtained, considering only the base grid-connected topology.

Table 15 presents the operating time of DOCRs in islanded mode and Topology 3 according to settings under Scenario 3. The decrements in operating times of DOCRs are considerable under Scenario 3 compared to Scenario 1. The comparative test

TABLE 29 Optimized settings and operating times of DOCRs in Topology 3 under Scenario 9

Main relay	TDS (s)	PCS (A)	CS	I_{HS} (A)	Backup relay	Topology 3		
						MROT (s)	BROT (s)	CTI (s)
1	0.546	55.54	EI	3574	NB	0.416	—	—
2	0.008	20.75	EI	3555	4	0.366	1.245	0.878
3	0.115	29.75	EI	3451	1	0.228	1.249	1.022
4	0.255	88.89	EI	3449	6	0.020	1.289	1.269
4	0.255	88.89	EI	3449	12	0.020	1.450	1.430
5	0.475	57.84	VI	3929	3	0.416	1.921	1.505
5	0.475	57.84	EI	3929	12	0.416	1.581	1.165
6	0.117	121.06	EI	7197	8	0.303	1.730	1.426
7	0.201	107.19	EI	4257	5	0.020	1.842	1.822
8	0.110	29.31	VI	4355	10	0.509	1.938	1.429
9	0.050	26.90	EI	3562	7	0.020	1.672	1.652
10	0.111	47.07	EI	4160	NB	0.393	—	—
11	1.049	128.64	EI	3305	3	0.020	1.391	1.371
11	1.049	128.64	EI	3305	6	0.020	1.387	1.367
12	0.554	46.33	EI	3970	14	0.675	1.396	0.721
13	1.250	152.65	NI	3673	11	0.020	1.287	1.267
14	0.511	61.42	EI	2896	16	0.481	1.562	1.081
15	0.093	78.50	NI	4154	13	0.020	1.649	1.629
16	0.282	76.18	NI	3874	18	0.298	1.463	1.164
17	0.139	41.60	VI	3198	15	0.020	1.873	1.853
18	1.095	236.74	EI	3596	20	0.310	1.689	1.379
18	1.095	236.74	EI	3596	22	0.310	1.902	1.592
19	0.007	85.05	EI	3994	17	0.020	1.762	1.742
19	0.007	85.05	EI	3994	22	0.020	1.906	1.886
20	0.064	98.79	VI	3031	NB	0.688	—	—
21	0.007	82.05	EI	3766	17	0.327	1.328	1.000
21	0.007	82.05	EI	3766	20	0.327	1.265	0.937
22	0.108	127.64	VI	3573	NB	0.675	—	—

TABLE 30 Operating times of relays 4 and 6 based on the proposed method and under various topologies for 3-phase short circuit

Resistance	Fault location 3-phase short circuit	Operating time (s) in Topology 1			Operating time (s) in Topology 2			Operating time (s) in Topology 3		
		R4	R6	CTI	R4	R6	CTI	R4	R6	CTI
$R = 0$	10%	0.020	1.979	1.959	0.020	1.542	1.522	0.020	1.455	1.435
	50%	0.020	2.176	2.156	0.020	1.928	1.908	0.020	1.656	1.636
	90%	0.020	2.644	2.624	1.103	3.124	2.021	0.020	1.998	1.978
$R = 1\ \Omega$	10%	0.020	2.074	2.054	0.020	1.740	1.7200	0.020	1.732	1.712
	50%	0.020	2.405	2.385	0.020	1.980	1.960	0.020	2.005	1.985
	90%	0.020	2.669	2.649	1.263	3.615	2.352	0.020	2.462	2.442
$R = 8\ \Omega$	10%	0.322	5.602	5.280	0.799	15.491	14.692	0.528	9.698	9.170
	50%	0.343	5.998	5.655	0.853	16.705	15.852	0.563	10.416	9.853
	90%	0.368	6.491	6.123	0.920	18.238	17.318	0.606	11.313	10.707

TABLE 31 Operating times of relays 4 and 6 based on the proposed method and under various topologies for 2-phase short circuit

Resistance	Fault location 2-phase short circuit	Operating time (s) in Topology 1			Operating time (s) in Topology 2			Operating time (s) in Topology 3		
		R4	R6	CTI	R4	R6	CTI	R4	R6	CTI
$R = 0$	10%	0.020	2.628	2.608	0.020	2.069	2.049	0.020	1.926	1.906
	50%	0.020	2.891	2.871	0.926	2.595	1.669	0.020	2.193	2.173
	90%	0.020	3.516	3.496	1.467	4.249	2.782	0.020	2.648	2.628
$R = 1\ \Omega$	10%	0.020	2.755	2.735	0.928	2.600	1.672	0.020	2.295	2.275
	50%	0.020	3.038	3.018	1.152	3.274	2.122	0.020	2.648	2.628
	90%	0.020	3.555	3.535	1.557	4.531	2.974	0.210	3.486	3.276
$R = 8\ \Omega$	10%	1.139	23.512	22.373	2.047	50.280	48.233	1.553	34.622	33.069
	50%	1.218	25.496	24.278	2.193	55.527	53.334	1.662	37.830	36.168
	90%	1.315	28.032	26.717	2.374	62.516	60.142	1.797	40.010	38.213

results show that optimizing the relay characteristics and HSRs improves the protective scheme's performance.

The considerable coordination constraint violations under Scenario 3 in islanded mode and Topology 3 illustrate the importance of considering various network configurations and related constraints in the optimization problem.

Figure 12 depicts the coordination curves of typical DOCRs (Relays 4 and 6) in the base configuration, islanded mode, and Topology 3 according to DIgSILENT protection simulations based on optimized settings under Scenario 3. As revealed by Figure 12, the time interval between the operating times of main and backup relays does not satisfy the selectivity constraints in islanded mode and Topology 3. The supplementary simulations in DIgSILENT approve the calculations in the proposed study.

The summary of selectivity constraints under Scenarios 1–3 has been demonstrated in Table 16. The presented results in Table 16 emphasize that it is necessary to concern the various network configurations in designing the SG's protection scheme because the SGs are allowed to operate in grid-connected/islanded mode and other configurations.

Table 17 presents the optimized settings and operating times of DOCRs under Scenario 4, where all configurations and corresponding constraints have been considered in one optimization problem. Table 18 shows the operating times of DOCRs in islanded mode and Topology 3 under Scenario 4. It is concluded that it is possible to mitigate the selectivity constraint violations using the solutions under Scenario 4. However, the operating times of DOCRs have increased under Scenario 4 compared to Scenario 1.

Figure 13 shows the results of DIgSILENT simulations based on the optimized settings for typical relays (4 and 6) under Scenario 4. The simulation results approve the accuracy of the proposed method and calculations. Also, comparing the time intervals between relays 4 and 6 under Scenarios 4 and 1 illustrates the advantages of considering various network configurations in the optimization problem. Although the operating times of DOCRs increase under Scenario 4, the probable coordination constraint violations are omitted.

Table 19 presents the optimal setting of DOCRs under Scenario 5. As discussed, under Scenario 5, one set of settings is applied to all DOCRs to protect the smart grids in various topologies. Optimizing the relay curves is the main difference between this scenario and Scenario 4. Also, comparing this scenario and Scenario 2 without considering different configurations in finding the optimized settings would be helpful.

In Table 20, the operating times and CTIs between the primary and backup relays in islanded mode and Topology 3 under Scenario 5 have been demonstrated. It is concluded that there is no coordination constraint violation under Scenario 5. The operating times have been improved compared to Scenario 4 because of optimal relay curves. However, a significant increment in operating times of DOCRs has occurred compared to Scenario 2, which is inevitable. If the system has not been equipped with communication systems and modernized relays, it is appropriate to apply the optimal settings under Scenarios 4–6.

In Figure 14, the results of DIgSILENT simulations based on the optimized settings for typical relays (4 and 6) under Scenario 5 have been shown. The simulation results approve the accuracy of the proposed method and calculations. Also, comparing the time intervals between relays 4 and 6 under Scenarios 5 and 2 illustrates the advantages of considering various network configurations in the optimization problem. Although the operating times of DOCRs increase under Scenario 5, the probable coordination constraint violations are omitted.

Table 21 shows the optimized settings for DOCRs under Scenario 6, while the relay curves have been optimized and HSRs have been used. Also, all network configurations have been concerned with the optimization problem under Scenario 6. In Table 22, the operating times of relays in islanded mode and Topology 3 have been presented. As seen, there is no selectivity constraint violation under Scenario 6 in islanded mode and Topology 3. Moreover, the advantages of optimal curves and HSRs have been highlighted based on comparative test results with Scenarios 4 and 5.

Figure 15 depicts the simulations in DIgSILENT for relays 4 and 6 under Scenario 6 in various network operation modes. Simulation results infer that these two typical relays are coordinated in various network topologies.

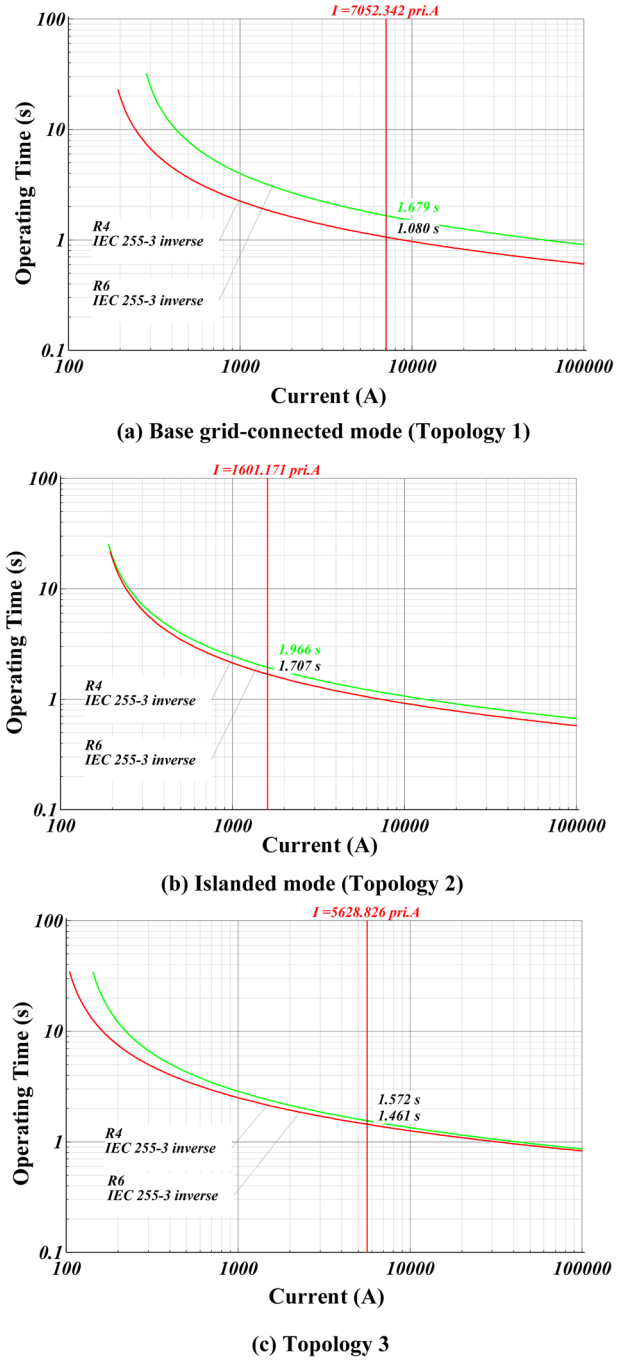

FIGURE 10 Coordination diagram of Relays 4 and 6 based on optimized settings under Scenario 1; (a) base grid-connected mode (Topology 1), (b) islanded mode (Topology 2), and (c) Topology 3

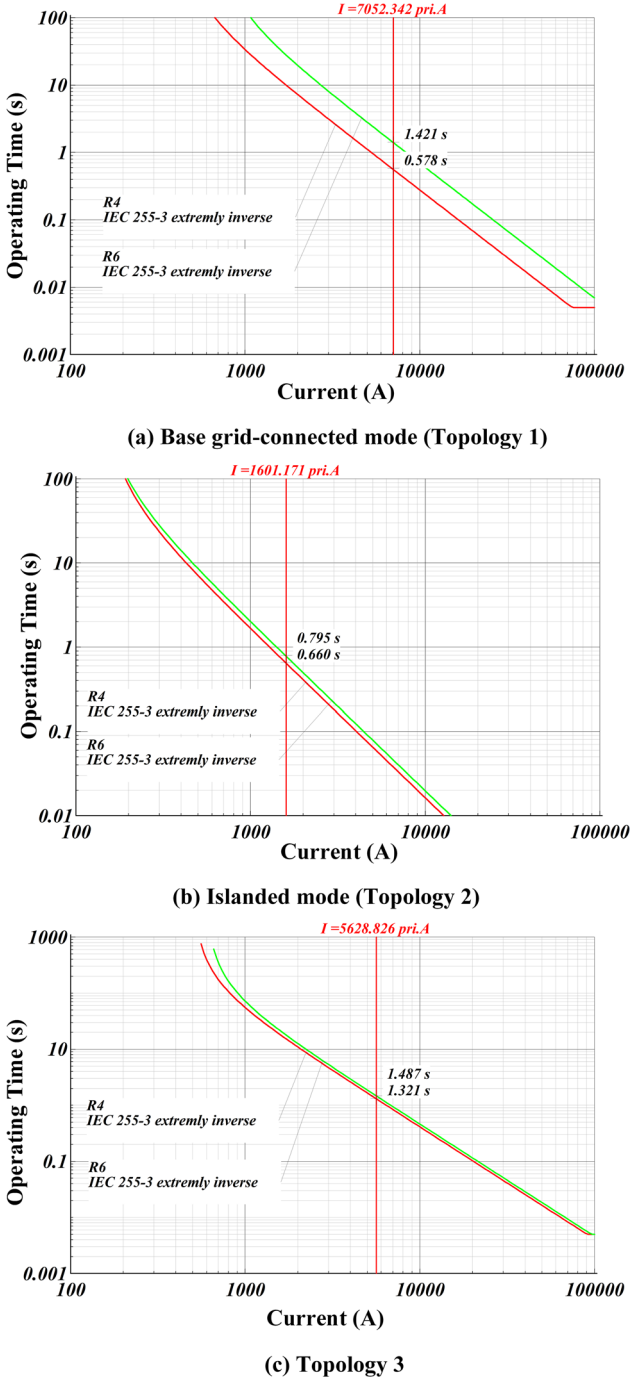

FIGURE 11 Coordination diagram of Relays 4 and 6 based on optimized settings under Scenario 2; (a) base grid-connected mode (Topology 1), (b) islanded mode (Topology 2), and (c) Topology 3

Table 23 shows the optimized settings of DOCRs under Scenario 7 in base network configurations. As discussed, an adaptive protection scheme is studied under Scenario 7. Hence, separate sets of settings are applied to DOCRs in different network configurations. The operating times and CTIs in other configurations have been demonstrated in Table 24.

Figure 16 shows the simulation results in DIgSILENT according to Scenario 7 for two typical relays (4 and 6). As seen, the required time interval exists between the operating times of primary and backup relays in different topologies.

As shown in Table 25, there is no coordination violation between the primary and backup relays under Scenario 7 in different topologies. The advantages of the adaptive protective scheme have been highlighted by comparing test results under various scenarios. It should be noted that the speed of the protective scheme under Scenario 7 is more than in Scenario 4. The

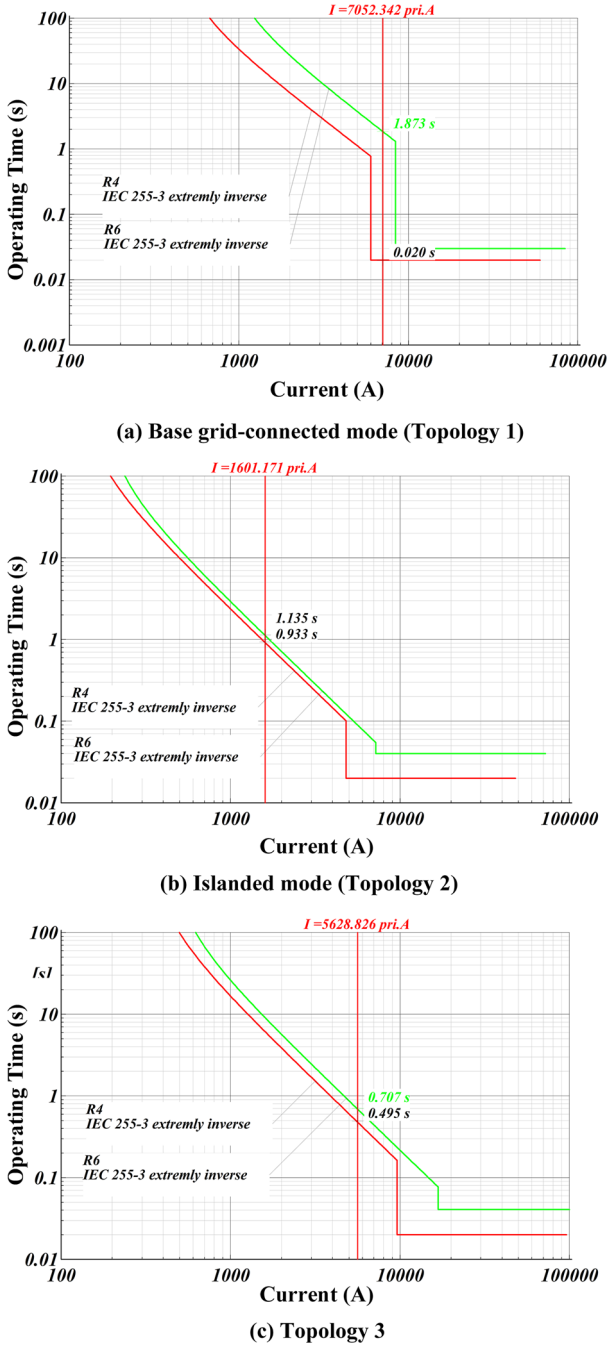

FIGURE 12 Coordination diagram of Relays 4 and 6 based on optimized settings under Scenario 3; (a) base grid-connected mode (Topology 1), (b) islanded mode (Topology 2), and (c) Topology 3

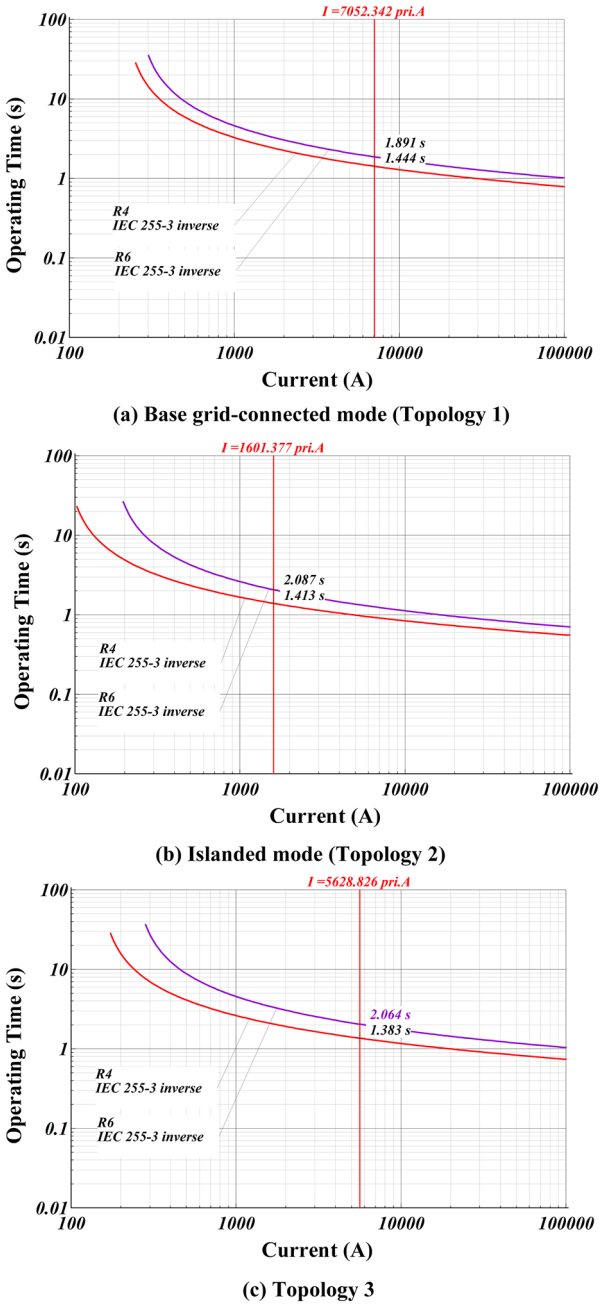

FIGURE 13 Coordination diagram of Relays 4 and 6 based on optimized settings under Scenario 4; (a) base grid-connected mode (Topology 1), (b) islanded mode (Topology 2), and (c) Topology 3

protective scheme's performance improvements under Scenario 7 are because of different settings for various network topologies. Indeed, better solutions could be found in the adaptive scheme because the feasible area of the optimization problem is extended by decreasing the constraints.

Table 25 shows the optimized settings of DOCRs under Scenario 8 in base network configurations. As discussed, an adaptive protection scheme is studied under Scenario 7. Hence, separate sets of settings are applied to DOCRs in different network configurations. Under this scenario, the optimal curves have been assigned to DOCRs in the adaptive scheme. The operating times and CTIs in other configurations have been demonstrated in Table 26.

Test results illustrate that the performance of the SG's protection schemes could be improved by optimizing the relay characteristics. The EI and VI characteristics have been assigned to DOCRs under Scenario 8. Studying the operating times of relays under Scenario 8 in different network configurations shows that the coordination constraint violations have been mitigated.

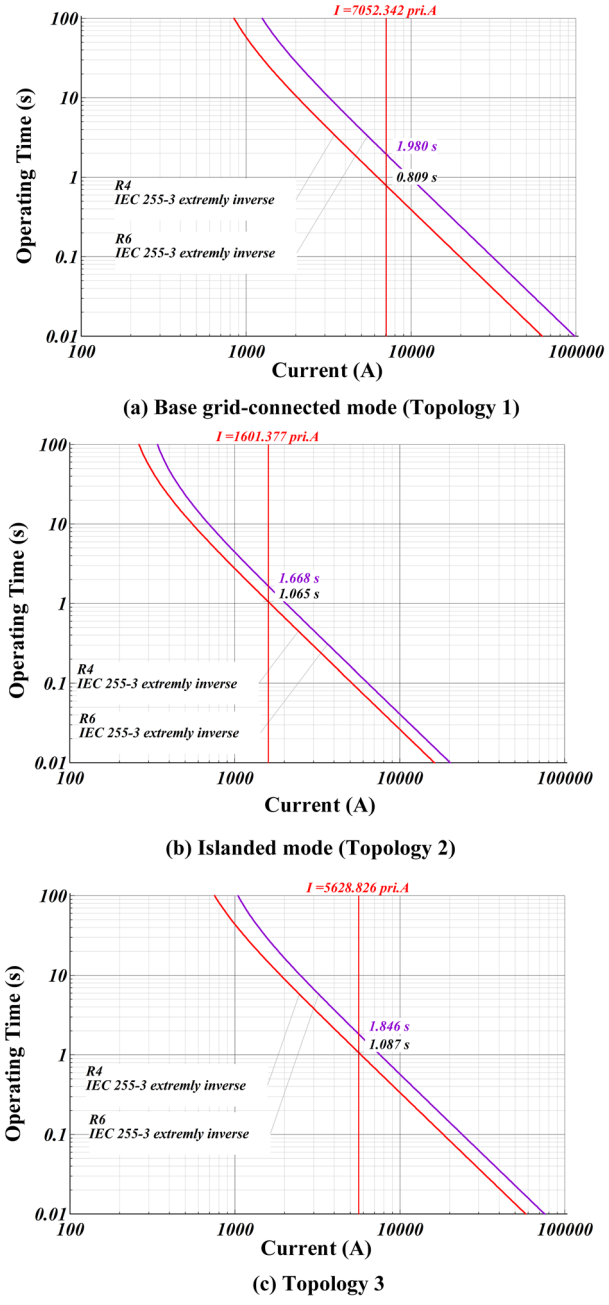

FIGURE 14 Coordination diagram of Relays 4 and 6 based on optimized settings under Scenario 5; (a) base grid-connected mode (Topology 1), (b) islanded mode (Topology 2), and (c) Topology 3

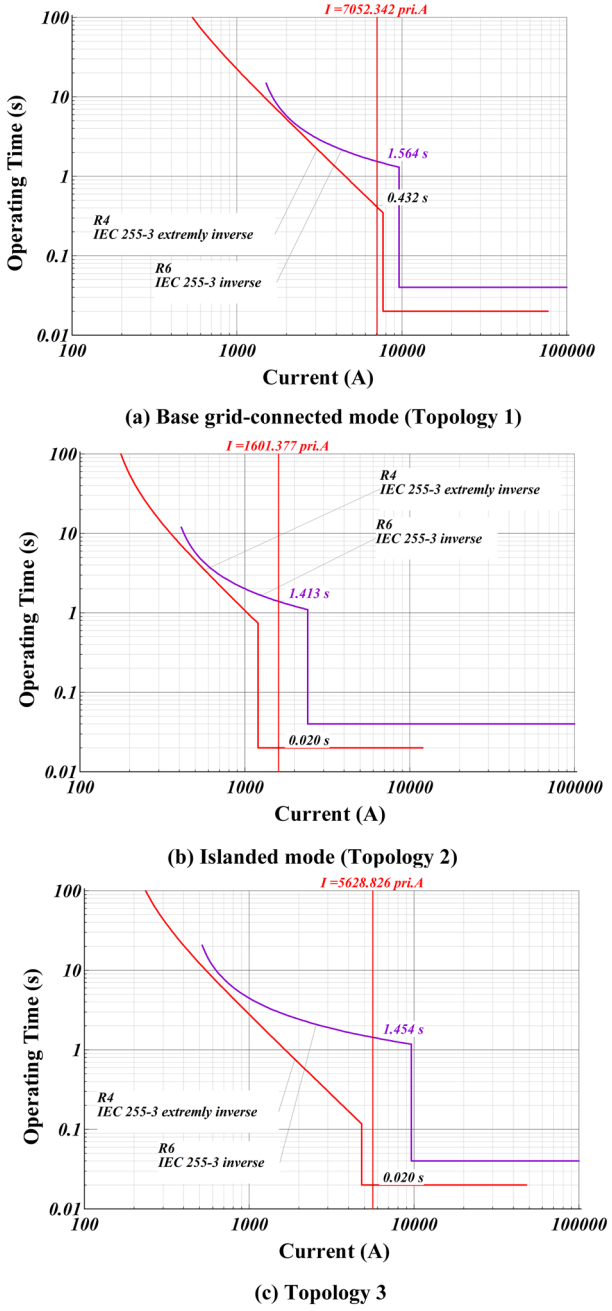

FIGURE 15 Coordination diagram of Relays 4 and 6 based on optimized settings under Scenario 6; (a) base grid-connected mode (Topology 1), (b) islanded mode (Topology 2), and (c) Topology 3

Figure 17 shows the simulation results in DIgSILENT according to Scenario 8 for two typical relays (4 and 6). As seen, the required time interval exists between primary and backup relays' operating times in different topologies. The operating times of main and backup relays have been decreased under Scenario 8 compared to Scenario 7. The simulations in DIgSILENT infer that optimizing the relay characteristic could be an appropriate solution to improve the protection of smart grids.

The convergence diagrams of solving the proposed optimization problem under Scenario 9 corresponding to various network configurations have been shown in Figure 18. The optimum values of the OF have been shown in convergence diagrams. Moreover, statistical analyses have been done to guarantee that obtained results are global optima and repetitive.

The optimized settings of DOCRs, including the current and time settings, relay curves, and HSRs' settings, for various network configurations have been shown in Tables 27–29. In the proposed adaptive protective scheme (Scenario 9), different sets of settings are applied to DOCRs based on the status of DGs and upstream networks. Comparing the operating times of DOCRs in various network topologies with other scenarios illustrates the advantages of the proposed method.

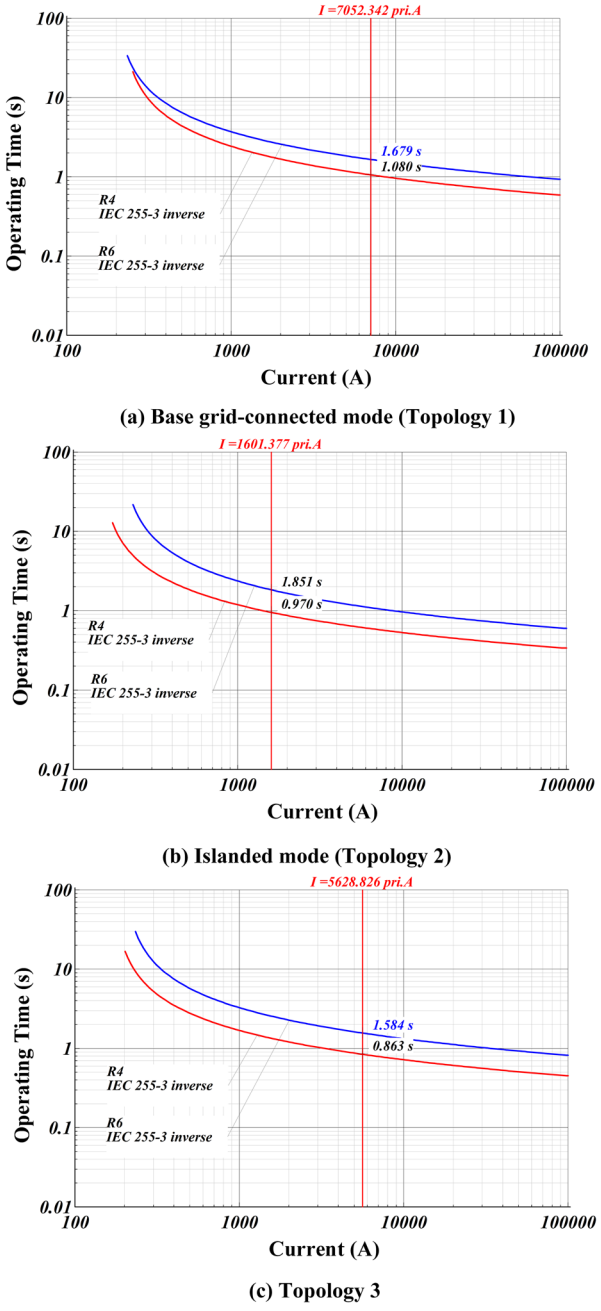

FIGURE 16 Coordination diagram of Relays 4 and 6 based on optimized settings under Scenario 7; (a) base grid-connected mode (Topology 1), (b) islanded mode (Topology 2), and (c) Topology 3

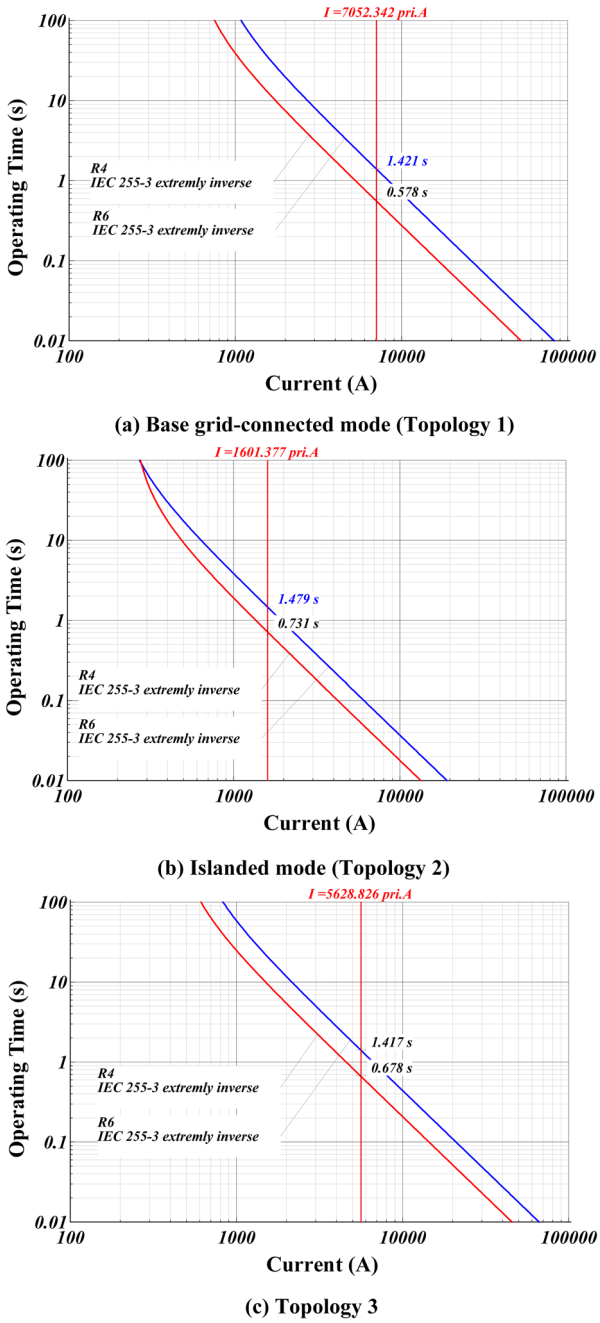

FIGURE 17 Coordination diagram of Relays 4 and 6 based on optimized settings under Scenario 8; (a) base grid-connected mode (Topology 1), (b) islanded mode (Topology 2), and (c) Topology 3

In the proposed adaptive protection scheme, based on optimal relay curves and HSRs, there is no coordination constraint violation, while the speed of the protective scheme is desired. The simultaneous benefits of adaptive schemes, optimal relay characteristics, and HSRs have improved the proposed method effectively.

Figure 19 depicts the protection studies for two typical DOCRs (Relays 4 and 6) in DIgSILENT based on the obtained results by the proposed protective scheme (Scenario 9). Simulation results are used to examine the accuracy of calculations in the proposed optimization problem. Simulation results infer that the coordination constraints have been satisfied in the proposed optimization problem.

3.6 | Sensitivity analysis

The amount of fault resistance, type of fault (fault phases), and fault distance to the relay location are effective parameters that can affect the performance of the proposed protection system. Therefore, in the sensitivity analysis, the performance of

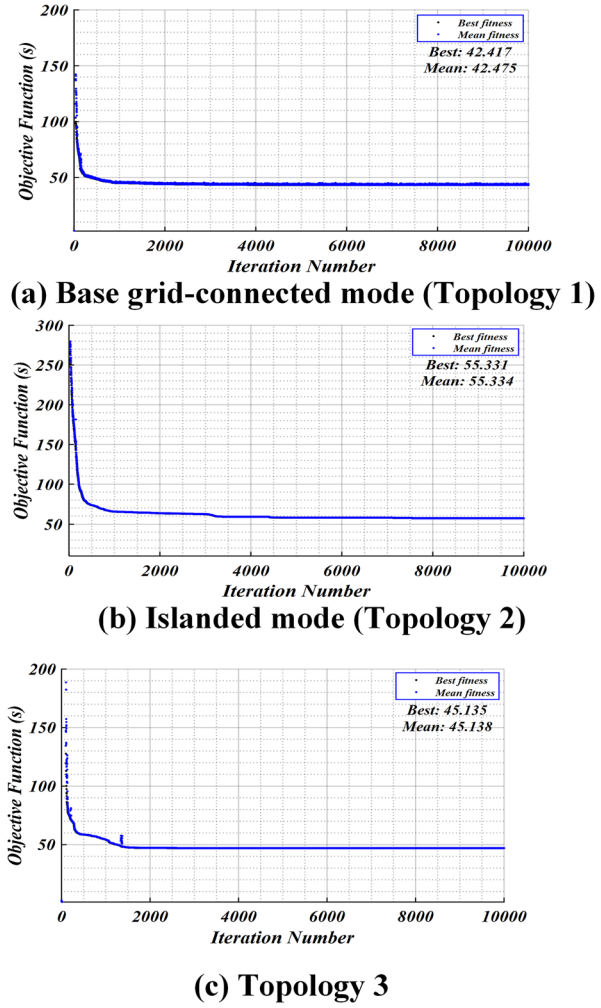

FIGURE 18 Convergence diagram of optimization problem solving by the GA under Scenario 9; (a) base grid-connected mode (Topology 1), (b) islanded mode (Topology 2), and (c) Topology 3

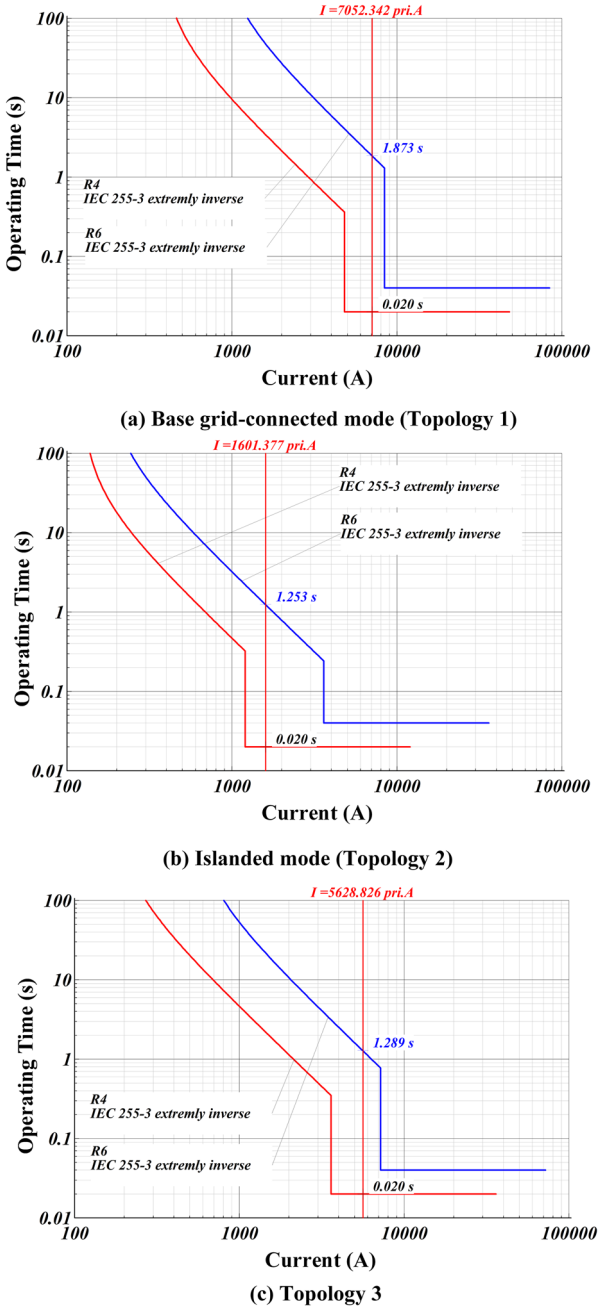

FIGURE 19 Coordination diagram of Relays 4 and 6 based on optimized settings under Scenario 9; (a) base grid-connected mode (Topology 1), (b) islanded mode (Topology 2), and (c) Topology 3

the protection system against changes in these parameters has been evaluated. Sensitivity analyses show that the performance of the proposed scheme (under Scenario 9) has good robustness against changes in the mentioned parameters.

To validate and analyze the proposed method, it has been examined for different types of faults and locations. For example, the sensitivity analysis results for two typical relays (relays 4 and 6) have been presented. In Table 30, the results of investigations for 3-phase faults in different network topologies and at different locations have been reported. Also, in Table 31, the test results for two-phase faults are shown.

As can be seen, the operating time of the relays increases by moving the fault location from near the relay (10% of the line) to a distance from the relay (90% of the line). In this case, the time interval between these relays satisfies the selectivity constraints, and because of the use of HSRs, the speed of the primary protection operation is desirable.

It has been tried to show that the obtained results are robust against the fault current changes due to changes in the fault location and impacts of fault resistance. The sensitivity analysis has been performed via changes in the fault resistance, and test results implied that up to 8 Ohm, the selectivity constraints based on optimized settings would be met. On the other hand, the 8 Ohm is a significant value representing the high impedance faults compared to load impedances.

4 | CONCLUSION

Although different studies have been done in the field of optimal protection of smart grids, there is a research gap in

developing an adaptive protective scheme, considering different network operations, with simultaneous optimal selection of relay characteristics and HSRs. This paper has tried to fill such a research gap. The proposed method has been developed based on using different sets of settings for various network configurations, while the optimized relay characteristics have been assigned to DOCRs. The proposed method has also been improved by using the HSRs. In this article, there is no coordination constraint violation by taking into account the different modes of network operation, while the speed of the protection system is appropriate. Also, the use of a high-set stage for DOCRs has been studied, which has greatly improved the performance speed of the relays, particularly the main relays, against the considerable short circuit currents. The introduced method has been applied to the distribution portion of the IEEE 38-bus test system. The comparative test results illustrated that a 31.78% and 21.62% decrement in time of the protective scheme in different topologies for the distribution networks of the IEEE 38-bus and IEEE 14-bus test systems could be achievable by simultaneous optimization of relay characteristics and HSRs compared to existing approaches, which used an adaptive protection scheme with pre-defined relay characteristics and without HSRs.

Extending the proposed study based on stability-oriented protection coordination will be one of the interesting future research works because the DGs are usually low-inertia machines in the ADNs, MGs, and SGs. Clustering the network configurations within the proposed adaptive protection scheme is another useful issue than can be developed in further works to support the numerous configurations.

NOMENCLATURE

Indices

i, m	Index of main relay
b, j	Index of backup relay
s	Index of network configuration

Parameters

OF	Objective function
T_s	Total operating time of main and backup relays in different operating modes
N_s	Number of different operating modes
s	Different configurations and operating modes
$TDS_{s,i}$	Time dial setting of the i-th relay in the s-th configuration
$PCS_{s,i}$	Pick-up current setting of the i-th relay in the s-th configuration
$CS_{s,i}$	Characteristic curve type of the i-th relay in the s-th configuration
$I_{s,i}^{HS}$	High set element setting value of the i-th relay in the s-th configuration
$t_{s,i}^{HS}$	High set element operating time in the s-th configuration
N_p	Number of primary relays
N_b	Number of backup relays
$t_{s,i}$	Operating time of the i-th primary relay under the s-th configuration
$t_{s,j}$	Operating time of the j-th backup relay under the s-th configuration
$k_{s,i}$and $n_{s,i}$	Standard relay characteristic's coefficient of the i-th relay in the s-th configuration
$t_{s,i}$	Operating time of the i-th relay in the s-th configuration
$I_{s,i}^{F}$	Fault current of the i-th relay in the s-th configuration
$TDS_{s,i}^{\min}$	Minimum permitted time dial setting of the i-th relay in the s-th configuration
$TDS_{s,i}^{\max}$	Maximum permitted time dial setting of the i-th relay in the s-th configuration
$PCS_{s,i}^{\min}$	Minimum permitted Pick-up current setting of the i-th relay in the s-th configuration
$PCS_{s,i}^{\max}$	Maximum permitted Pick-up current setting of the i-th relay in the s-th configuration
$I_{s,i}^{Load,\max}$	Maximum current flowing through the i-th relay in the s-th configuration
$I_{s,i}^{F,\min}$	Minimum fault current flowing through the i-th relay in the s-th configuration
$I_{s,i}^{HS,\min}$	Minimum permitted high set element i-th relay in the s-th configuration
$I_{s,i}^{HS,\max}$	Maximum permitted high set element i-th relay in the s-th configuration
$t_{s,i}^{HS,\min}$	Minimum permitted high set element for the i-th relay in the s-th configuration
$t_{s,i}^{HS,\max}$	Maximum permitted high set element for the i-th relay in the s-th configuration
CTI	Minimum coordination interval between main and backup relay
$PCS^{\min}$	Minimum pickup current setting of relays based on manufacturer's specifications
$PCS^{\max}$	Maximum pickup current setting of relays based on manufacturer's specifications

Abbreviations

OF	Objective function
GA	Genetic algorithm
DOCR	Directional overcurrent relay
DG	Distribution generation
NB	No backup relay
MROT	Main relay's operating time
BROT	Backup relay's operating time
SG	Smart grid
MG	Microgrid
ADN	Active distribution network
HSR	High-set relay
NI	Normally inverse
VI	Very inverse
EI	Extremely inverse
TDS	Time dial setting
PCS	Pickup current setting
CS	Curve setting

CTI Coordination time interval
SLD Single line diagram

DATA AVAILABILITY STATEMENT

Data available on request from the authors.

CONFLICT OF INTEREST

The authors declare that they have no known competing financial interests or personal relationships that could have appeared to influence the work reported in this paper.

FUNDING INFORMATION

The authors received no funding for this article.

AUTHOR CONTRIBUTIONS

H.H.-D.: Conceptualization; Formal analysis; Investigation; Methodology; Project administration; Software; Supervision; Validation; Writing—Original draft; Writing—Review and editing. A.K.: Conceptualization; Investigation; Methodology; Project administration; Supervision; Validation; Writing—Review and editing

ORCID

Hamed Hashemi-Dezaki https://orcid.org/0000-0003-2056-2388

REFERENCES

1. Eghbali N., Hakimi S.M., Hasankhani A., Derakhshan G., Abdi B.: Stochastic energy management for a renewable energy based microgrid considering battery, hydrogen storage, and demand response. Sustainable Energy Grids Networks 30, 100652 (2022), https://doi.org/10.1016/j.segan.2022.100652
2. Sarangi S., Sahu B.K., Rout P.K.: Review of distributed generator integrated AC microgrid protection: Issues, strategies, and future trends. Int. J. Energy Res. 45(10), 14117–14144 (2021), https://doi.org/10.1002/er.6689
3. El-Naily N., Saad S.M., Hussein T., Mohamed F.A.: A novel constraint and non-standard characteristics for optimal over-current relays coordination to enhance microgrid protection scheme. IET Gener. Transm. Distrib. 13(6), 780–793 (2019), https://doi.org/10.1049/iet-gtd.2018.5021
4. Hakimi S.M., Hasankhani A., Shafie-khah M., Lotfi M., Catalão J.P.S.: Optimal sizing of renewable energy systems in a Microgrid considering electricity market interaction and reliability analysis. Electr. Power Syst. Res. 203, 107678 (2022), https://doi.org/10.1016/j.epsr.2021.107678
5. Lei J., Gong Q.: Optimal allocation of a hybrid energy storage system considering its dynamic operation characteristics for wind power applications in active distribution networks. Int. J. Energy Res. 42(13), 4184–4196 (2018), https://doi.org/10.1002/er.4164
6. Hojjaty M., Fani B., Sadeghkhani I.: Intelligent protection coordination restoration strategy for active distribution networks. IET Gener. Transm. Distrib. 16(3), 397–413 (2022), https://doi.org/10.1049/gtd2.12238
7. Sarangi S., Sahu B.K., Rout P.K.: Distributed generation hybrid AC/DC microgrid protection: A critical review on issues, strategies, future directions. Int. J. Energy Res. 44(5), 3347–3364 (2020), https://doi.org/10.1002/er.5128
8. Abd-Elkader A.G., Saleh S.M.: Zero non-detection zone assessment for anti-islanding protection in rotating machines based distributed generation system. Int. J. Energy Res. 45(1), 521–540 (2021), https://doi.org/10.1002/er.5705
9. Tiwari S.P., Koley E., Ghosh S.: Communication-less ensemble classifier-based protection scheme for DC microgrid with adaptiveness to network reconfiguration and weather intermittency. Sustainable Energy Grids Networks 26, 100460 (2021), https://doi.org/10.1016/j.segan.2021.100460
10. Ghotbi-Maleki M., Mohammadi Chabanloo R., Taheri M.R., Zeineldin H.H.: Coordination of non-directional overcurrent relays and fuses in active distribution networks considering reverse short-circuit currents of DGs. IET Gener. Transm. Distrib. 15(18), 2539–2553 (2021), https://doi.org/10.1049/gtd2.12197
11. Sampaio F.C., Tofoli F.L., Melo L.S., Barroso G.C., Sampaio R.F., Leão R.P.S.: Adaptive fuzzy directional bat algorithm for the optimal coordination of protection systems based on directional overcurrent relays. Electr. Power Syst. Res. 211, 108619 (2022), https://doi.org/10.1016/j.epsr.2022.108619
12. Sharma A., Kiran D., Panigrahi B.K.: Planning the coordination of overcurrent relays for distribution systems considering network reconfiguration and load restoration. IET Gener. Transm. Distrib. 12(7), 1672–1679 (2018), https://doi.org/10.1049/iet-gtd.2017.1674
13. Azari M., Mazlumi K., Ojaghi M.: Efficient non-standard tripping characteristic-based coordination method for overcurrent relays in meshed power networks. Electr. Eng. 104(4), 2061–2078 (2022), https://doi.org/10.1007/s00202-021-01459-3
14. Sadeghi M.H., Dastfan A., Damchi Y.: Optimal distributed generation penetration considering relay coordination and power quality requirements. IET Gener. Transm. Distrib. 16(12), 2466–2475 (2022), https://doi.org/10.1049/gtd2.12466
15. Ghotbi Maleki M., Mohammadi Chabanloo R., Farrokhifar M.: Accurate coordination method based on the dynamic model of overcurrent relay for industrial power networks taking contribution of induction motors into account. IET Gener. Transm. Distrib. 14(4), 645–655 (2020), https://doi.org/10.1049/iet-gtd.2019.0325
16. Baghaee H.R., Mirsalim M., Gharehpetian G.B., Talebi H.A.: MOPSO/FDMT-based Pareto-optimal solution for coordination of overcurrent relays in interconnected networks and multi-DER microgrids. IET Gener. Transm. Distrib. 12(12), 2871–2886 (2018), https://doi.org/10.1049/iet-gtd.2018.0079
17. Alam M.N., Das B., Pant V.: Protection coordination scheme for directional overcurrent relays considering change in network topology and OLTC tap position. Electr. Power Syst. Res. 185, 106395 (2020), https://doi.org/10.1016/j.epsr.2020.106395
18. Sadeghi S., Hashemi-Dezaki H., Entekhabi-Nooshabadi A.M.: Optimal protection scheme of micro-grids considering N−1 contingency by a new hybrid GA-PSO-LP optimization algorithm. In: *2021 11th Smart Grid Conference (SGC)*, Tabriz, Iran, pp. 1–5 (2021), https://doi.org/10.1109/SGC54087.2021.9664076
19. Jarrahi M.A., Samet H., Ghanbari T.: Protection framework for microgrids with inverter-based DGs: A superimposed component and waveform similarity-based fault detection and classification scheme. IET Gener. Transm. Distrib. 16(11), 2242–2264 (2022), https://doi.org/10.1049/gtd2.12438
20. Saleh K.A., Zeineldin H.H., El-Saadany E.F.: Optimal protection coordination for microgrids considering N−1 contingency. IEEE Trans. Ind. Inf. 13(5), 2270–2278 (2017), https://doi.org/10.1109/TII.2017.2682101
21. Sati T., Azzouz M.A.: Optimal protection coordination for inverter dominated islanded microgrids considering N−1 contingency. IEEE Trans. Power Delivery 37(3), 2256–2267 (2021), https://doi.org/10.1109/TPWRD.2021.3108760
22. Entekhabi-Nooshabadi A.M., Hashemi-Dezaki H., Taher S.A.: Optimal microgrid's protection coordination considering N−1 contingency and optimum relay characteristics. Appl. Soft Comput. 98, 106741 (2021), https://doi.org/10.1016/j.asoc.2020.106741
23. Ataee-Kachoee A.H., Hashemi-Dezaki H., Ketabi A.: Optimal protection coordination of dual-setting directional overcurrent relays based on three-point coordination strategy. In: *2021 11th Smart Grid Conference (SGC)*, Tabriz, Iran, pp. 1–6 (2021), https://doi.org/10.1109/SGC54087.2021.9664089
24. Ataee-Kachoee A.H., Hashemi-Dezaki H., Ketabi A.: Optimal protective coordination of microgrids considering N−1 contingency using dual characteristics directional overcurrent relays. In: 2022 International Conference on Protection and Automation of Power Systems (IPAPS), Zahedan, Iran, pp. 1–10 (2022), https://doi.org/10.1109/IPAPS55380.2022.9763257

25. Azari M., Mazlumi K., Ojaghi M.: Optimal directional overcurrent relay coordination in interconnected networks considering user-defined PWL characteristic curve. Arabian J. Sci. Eng. 47(3), 3119–3139 (2022), https://doi.org/10.1007/s13369-021-06048-x
26. Anand A., Affijulla S.: Ensemble empirical mode decomposition-based differential protection scheme for islanded and grid-tied AC microgrid. IET Gener. Transm. Distrib. 14(26), 6674–6681 (2020), https://doi.org/10.1049/iet-gtd.2020.1117
27. Tadikonda N., Kumar J., Mahanty R.N.: A technique for detection of islanding in a microgrid on the basis of rate of change of superimposed impedance (ROCSI). Electr. Power Syst. Res. 206, 107838 (2022), https://doi.org/10.1016/j.epsr.2022.107838
28. El-Hamrawy A.H., Ebrahiem A.A.M., Megahed A.I.: Improved adaptive protection scheme based combined centralized/decentralized communications for power systems equipped with distributed generation. IEEE Access 10, 97061–97074 (2022), https://doi.org/10.1109/ACCESS.2022.3205312
29. Tajdinian M., Khosravi H., Samet H., Ali Z.M.: Islanding detection scheme using potential energy function based criterion. Electr. Power Syst. Res. 209, 108047 (2022), https://doi.org/10.1016/j.epsr.2022.108047
30. Allan O.A., Morsi W.G.: A new passive islanding detection approach using wavelets and deep learning for grid-connected photovoltaic systems. Electr. Power Syst. Res. 199, 107437 (2021), https://doi.org/10.1016/j.epsr.2021.107437
31. Hatata A.Y., Ebeid A.S., El-Saadawi M.M.: Optimal restoration of directional overcurrent protection coordination for meshed distribution system integrated with DGs based on FCLs and adaptive relays. Electr. Power Syst. Res. 205, 107738 (2022), https://doi.org/10.1016/j.epsr.2021.107738
32. Samadi A., Mohammadi Chabanloo R.: Adaptive coordination of overcurrent relays in active distribution networks based on independent change of relays' setting groups. Int. J. Electr. Power Energy Syst. 120, 106026 (2020), https://doi.org/10.1016/j.ijepes.2020.106026
33. Hatefi Torshizi N., Najafi H., Saberi Noghabi A., Sadeh J.: An adaptive characteristic for overcurrent relays considering uncertainty in presence of distributed generation. Int. J. Electr. Power Energy Syst. 128, 106688 (2021), https://doi.org/10.1016/j.ijepes.2020.106688
34. Sadeghi M.H., Dastfan A., Damchi Y.: Robust and adaptive coordination approaches for co-optimization of voltage dip and directional overcurrent relays coordination. Int. J. Electr. Power Energy Syst. 129, 106850 (2021), https://doi.org/10.1016/j.ijepes.2021.106850
35. Mohammadi R., Safari M., Gholizadeh-Roshanagh R.: Reducing the scenarios of network topology changes for adaptive coordination of overcurrent relays using hybrid GA-LP. IET Gener. Transm. Distrib. 12(21), 5897–5890 (2018), https://doi.org/10.1049/iet-gtd.2018.5810
36. Momesso A.E.C., Bernardes W.M.S., Asada E.N.: Adaptive directional overcurrent protection considering stability constraint. Electr. Power Syst. Res. 181, 106190 (2020), https://doi.org/10.1016/j.epsr.2019.106190
37. Uddin M.N., Rezaei N., Olufemi O.E.: Adaptive and optimal overcurrent protection of wind farms with improved reliability. IEEE Trans. Ind. Appl. 58(3), 3342–3352 (2022), https://doi.org/10.1109/TIA.2022.3147151
38. Yousaf M., Jalilian A., Muttaqi K.M., Sutanto D.: An adaptive overcurrent protection scheme for dual-setting directional recloser and fuse coordination in unbalanced distribution networks with distributed generation. IEEE Trans. Ind. Appl. 58(2), 1831–1842 (2022), https://doi.org/10.1109/TIA.2022.3146095
39. Purwar E., Vishwakarma D.N., Singh S.P.: A novel constraints reduction-based optimal relay coordination method considering variable operational status of distribution system with DGs. IEEE Trans. Smart Grid 10(1), 889–898 (2019), https://doi.org/10.1109/TSG.2017.2754399
40. Narimani A., Hashemi-Dezaki H.: Optimal stability-oriented protection coordination of smart grid's directional overcurrent relays based on optimized tripping characteristics in double-inverse model using high-set relay. Int. J. Electr. Power Energy Syst. 133, 107249 (2021), https://doi.org/10.1016/j.ijepes.2021.107249
41. Dadfar S., Gandomkar M.: Augmenting protection coordination index in interconnected distribution electrical grids: Optimal dual characteristic using numerical relays. Int. J. Electr. Power Energy Syst. 131, 107107 (2021), https://doi.org/10.1016/j.ijepes.2021.107107
42. Yazdaninejadi A., Nazarpour D., Golshannavaz S.: Sustainable electrification in critical infrastructure: Variable characteristics for overcurrent protection considering DG stability. Sustainable Cities Soc. 54, 102022 (2020), https://doi.org/10.1016/j.scs.2020.102022
43. Ahmadi S.A., Karami H., Sanjari M.J., Tarimoradi H., Gharehpetian G.B.: Application of hyper-spherical search algorithm for optimal coordination of overcurrent relays considering different relay characteristics. Int. J. Electr. Power Energy Syst. 83, 443–449 (2016), https://doi.org/10.1016/j.ijepes.2016.04.042
44. Alam M.N.: Overcurrent protection of AC microgrids using mixed characteristic curves of relays. Comput. Electr. Eng. 74, 74–88 (2019), https://doi.org/10.1016/j.compeleceng.2019.01.003
45. Hemmati R., Mehrjerdi H.: Non-standard characteristic of overcurrent relay for minimum operating time and maximum protection level. Simul. Modell. Pract. Theory 97, 101953 (2019), https://doi.org/10.1016/j.simpat.2019.101953
46. El-Naily N., Saad S.M., Mohamed F.A.: Novel approach for optimum coordination of overcurrent relays to enhance microgrid earth fault protection scheme. Sustainable Cities Soc. 54, 102006 (2020), https://doi.org/10.1016/j.scs.2019.102006
47. Saad S.M., El-Naily N., Mohamed F.A.: A new constraint considering maximum PSM of industrial over-current relays to enhance the performance of the optimization techniques for microgrid protection schemes. Sustainable Cities Soc. 44, 445–457 (2019), https://doi.org/10.1016/j.scs.2018.09.030
48. Elmitwally A., Kandil M.S., Gouda E., Amer A.: Mitigation of DGs impact on variable-topology meshed network protection system by optimal fault current limiters considering overcurrent relay coordination. Electr. Power Syst. Res. 186, 106417 (2020), https://doi.org/10.1016/j.epsr.2020.106417
49. Zeineldin H.H., Sharaf H.M., Ibrahim D.K., El-Zahab E.E.D.A.: Optimal protection coordination for meshed distribution systems with DG using dual setting directional over-current relays. IEEE Trans. Smart Grid 6(1), 115–123 (2015), https://doi.org/10.1109/TSG.2014.2357813
50. Kida A.A., Labrador Rivas A.E., Gallego L.A.: An improved simulated annealing–linear programming hybrid algorithm applied to the optimal coordination of directional overcurrent relays. Electr. Power Syst. Res. 181, 106197 (2020), https://doi.org/10.1016/j.epsr.2020.106197
51. Alam M.N.: Adaptive protection coordination scheme using numerical directional overcurrent relays. IEEE Trans. Ind. Inf. 15(1), 64–73 (2019), https://doi.org/10.1109/TII.2018.2834474
52. Ghotbi Maleki M., Mohammadi Chabanloo R., Taheri M.R.: Mixed-integer linear programming method for coordination of overcurrent and distance relays incorporating overcurrent relays characteristic selection. Int. J. Electr. Power Energy Syst. 110, 246–257 (2019), https://doi.org/10.1016/j.ijepes.2019.03.007
53. Mohammadi Chabanloo R., Ghotbi Maleki M.: An accurate method for overcurrent–distance relays coordination in the presence of transient states of fault currents. Electr. Power Syst. Res. 158, 207–218 (2018), https://doi.org/10.1016/j.epsr.2018.01.013
54. Aghdam T.S., Karegar H.K., Zeineldin H.H.: Optimal coordination of double-inverse overcurrent relays for stable operation of DGs. IEEE Trans. Ind. Inf. 15(1), 183–192 (2019), https://doi.org/10.1109/TII.2018.2808264
55. Dehghanpour E., Karegar H.K., Kheirollahi R., Soleymani T.: Optimal coordination of directional overcurrent relays in microgrids by using cuckoo-linear optimization algorithm and fault current limiter. IEEE Trans. Smart Grid 9(2), 1365–1375 (2018), https://doi.org/10.1109/TSG.2016.2587725
56. Naveen P., Jena P.: Adaptive protection scheme for microgrid with multiple point of common couplings. IEEE Syst. J. 15(4), 5618–5629 (2021), https://doi.org/10.1109/JSYST.2020.3039881
57. Mahat P., Chen Z., Bak-Jensen B., Bak C.L.: A simple adaptive overcurrent protection of distribution systems with distributed generation. IEEE Trans. Smart Grid 2(3), 428–437 (2011), https://doi.org/10.1109/TSG.2011.2149550

58. Erlich I., Winter W., Dittrich A.: Advanced grid requirements for the integration of wind turbines into the German transmission system. In: *2006 IEEE Power Engineering Society General Meeting*, Montreal, QC, Canada (2006), https://doi.org/10.1109/PES.2006.1709340
59. Sadeghi M.H., Dastfan A., Damchi Y.: Optimal distributed generation penetration considering relay coordination and power quality requirements. IET Gener. Transm. Distrib. 16(12), 2466–2475 (2022), https://doi.org/10.1049/gtd2.12466
60. Alam M.N., Gokaraju R., Chakrabarti S.: Protection coordination for networked microgrids using single and dual setting overcurrent relays. IET Gener. Transm. Distrib. 14(14), 2818–2828 (2020), https://doi.org/10.1049/iet-gtd.2019.0557
61. Ataei M.A., Gitizadeh M., Lehtonen M., Razavi-Far R.: Multi-agent based protection scheme using current-only directional overcurrent relays for looped/meshed distribution systems. IET Gener. Transm. Distrib. 16(8), 1567–1581 (2022), https://doi.org/10.1049/gtd2.12234
62. Ataei M.A., Gitizadeh M.: A distributed adaptive protection scheme based on multi-agent system for distribution networks in the presence of distributed generations. IET Gener. Transm. Distrib. 16(8), 1521–1540 (2022), https://doi.org/10.1049/gtd2.12351
63. Karimi H., Fani B., Shahgholian G.: Multi agent-based strategy protecting the loop-based micro-grid via intelligent electronic device-assisted relays. IET Renewable Power Gener. 14(19), 4132–4141 (2020), https://doi.org/10.1049/iet-rpg.2019.1233
64. Saldarriaga-Zuluaga S.D., López-Lezama J.M., Muñoz-Galeano N.: Optimal coordination of over-current relays in microgrids considering multiple characteristic curves. Alexandria Eng. J. 60(2), 2093–2113 (2021), https://doi.org/10.1016/j.aej.2020.12.012
65. Alam M.R., Muttaqi K.M., Bouzerdoum A.: Evaluating the effectiveness of a machine learning approach based on response time and reliability for islanding detection of distributed generation. IET Renewable Power Gener. 11(11), 1392–1400 (2017), https://doi.org/10.1049/iet-rpg.2016.0987
66. Wong J., Tan C., Bakar A.H.A., Che H.S.: Selectivity problem in adaptive overcurrent protection for microgrid with inverter-based distributed generators (IBDG): Theoretical investigation and HIL verification. IEEE Trans. Power Delivery 37(4), 3313–3324 (2021), https://doi.org/10.1109/TPWRD.2021.3126897
67. Sadeghi S., Hashemi-Dezaki H., Entekhabi-Nooshabadi A.M.: Optimized protection coordination of smart grids considering N−1 contingency based on reliability-oriented probability of various topologies. Electr. Power Syst. Res. 213, 108737 (2022), https://doi.org/10.1016/j.epsr.2022.108737
68. Ojaghi M., Mohammadi V.: Use of clustering to reduce the number of different setting groups for adaptive coordination of overcurrent relays. IEEE Trans. Power Delivery 33(3), 1204–1212 (2018), https://doi.org/10.1109/TPWRD.2017.2749321
69. Abbaspour E., Fani B., Karami-Horestani A.: Adaptive scheme protecting renewable-dominated micro-grids against usual topology-change events. IET Renewable Power Gener. 15(12), 2686–2698 (2021), https://doi.org/10.1049/rpg2.12193
70. Sharaf H. M., Zeineldin H. H., El-Saadany E.: Protection coordination for microgrids with grid-connected and islanded capabilities using communication assisted dual setting directional overcurrent relays. IEEE Trans. Smart Grid 9(1), 143–151 (2018), https://doi.org/10.1109/TSG.2016.2546961
71. Damchi Y., Dolatabadi M.: Hybrid VNS–LP algorithm for online optimal coordination of directional overcurrent relays. IET Gener. Transm. Distrib. 14(23), 5447–5455 (2020), https://doi.org/10.1049/iet-gtd.2019.1811
72. Kumar D. S., Srinivasan D., Sharma A., Reindl T.: Adaptive directional overcurrent relaying scheme for meshed distribution networks. IET Gener. Transm. Distrib. 12(13), 3212–3220 (2018), https://doi.org/10.1049/iet-gtd.2017.1279
73. Fani B., Bisheh H., Sadeghkhani I.: Protection coordination scheme for distribution networks with high penetration of photovoltaic generators. IET Gener. Transm. Distrib. 12(8), 1802–1814 (2018), https://doi.org/10.1049/iet-gtd.2017.1229
74. Yazdaninejadi A., Nazarpour D., Talavat V.: Optimal coordination of dual-setting directional over-current relays in multi-source meshed active distribution networks considering transient stability. IET Gener. Transm. Distrib. 13(2), 157–170 (2019), https://doi.org/10.1049/iet-gtd.2018.5431
75. *ABB REJ 532 Datasheet and Specifications*. https://new.abb.com/medium-voltage/digital-substations/protection-relay-services/legacy-relays-and-related-devices-and-tools/overcurrent-relay-rej-523. Accessed 2022
76. Zanjani M. G. M., Mazlumi K., Kamwa I.: Application of μPMUs for adaptive protection of overcurrent relays in microgrids. IET Gener. Transm. Distrib. 12(18), 4061–4068 (2018), https://doi.org/10.1049/iet-gtd.2018.5898
77. Darabi A., Bagheri M., Gharehpetian G.B.: Highly sensitive microgrid protection using overcurrent relays with a novel relay characteristic. IET Renewable Power Gener. 14(7), 1201–1209 (2020), https://doi.org/10.1049/iet-rpg.2019.0793
78. Saha D., Datta A., Das P.: Optimal coordination of directional overcurrent relays in power systems using Symbiotic Organism Search Optimisation technique. IET Gener. Transm. Distrib. 10(11), 2681–2688 (2016), https://doi.org/10.1049/iet-gtd.2015.0961
79. Ghadiri S.M.E., Mazlumi K.: Adaptive protection scheme for microgrids based on SOM clustering technique. Appl. Soft Comput. 88, 106062 (2020), https://doi.org/10.1016/j.asoc.2020.106062
80. Karimkhan Zand H., Mazlumi K., Bagheri A.: A new approach to the setting of directional overcurrent relays by incorporating cascading outages. Sci. Iran. 29(3), 1562–1572 (2022), 10.24200/sci.2020.54782.3916
81. Gabr M.A., El-Sehiemy R.A., Megahed T.F., Ebihara Y., Abdelkader S.M.: Optimal settings of multiple inverter-based distributed generation for restoring coordination of DOCRs in mesh distribution networks. Electr. Power Syst. Res. 213, 108757 (2022), https://doi.org/10.1016/j.epsr.2022.108757
82. Singh P., Pradhan A.K.: A Local measurement based protection technique for distribution system with photovoltaic plants. IET Renewable Power Gener. 14(6), 996–1003 (2020), https://doi.org/10.1049/iet-rpg.2019.0996
83. Aghaei H., Hashemi-Dezaki H.: Optimal communication-aided protection of meshed smart grids considering stability constraints of distributed generations incorporating optimal selection of relay characteristics. IET Renewable Power Gener. 16(11), 2313–2337 (2022), https://doi.org/10.1049/rpg2.12525
84. Fayazi H., Fani B., Moazzami M., Shahgholian G.: An offline three-level protection coordination scheme for distribution systems considering transient stability of synchronous distributed generation. Int. J. Electr. Power Energy Syst. 131, 107069 (2021), https://doi.org/10.1016/j.ijepes.2021.107069

How to cite this article: Ataee-Kachoee, A.H., Hashemi-Dezaki, H., Ketabi, A.: Optimal adaptive protection of smart grids using high-set relays and smart selection of relay tripping characteristics considering different network configurations and operation modes. IET Gener. Transm. Distrib. 16, 5084–5116 (2022). https://doi.org/10.1049/gtd2.12659